KODAIKANAL OBSERVATORY
BULLETIN Number 180

The Evershed Effect and Line Asymmetry in Sunspot Penumbrae

A. Bhatnagar

Abstract

During the two successive passages of a sunspot across the solar disk, velocity field configurations have been obtained using three Zeeman insensitive lines (g=o), 4912.027, NiI ; 5576.101, FeI and 5691.508 FeI (Ni). Large image resolution and high spectrographic dispersion have been used for the determination of sight-line velocities in the spot. The observed sight-line velocities have been resolved into three mutually perpendicular directions—the radial, tangential and the vertical components. The magnitude of the maximum radial velocity component, Umax, depends on the disc position of the spot and on the strength of the line. For lines of Rowland intensity 1, the magnitude of Umax, in the spot penumbrae near the disc centre is about 2.0 to 2.5 km/sec, directed radially outwards towards the photosphere. Well developed spots show large radial velocities compared to spots in the initial phases. From the knowledge of the mean depth of formation of lines in sunspot penumbrae (using Makita's sunspot penumbral model), a mean gradient of Umax with depth, of the order of 4×10^{-3} km/sec. per km. in depth, has been obtained.

Small vertical velocities of the order of 0.6 km/sec., and less, directed downwards in the penumbral region, have been observed.

Sizable tangential velocities of the order of 0.6 to 1.0 km/sec. in the spot penumbrae have been detected. No definite direction of rotational motion in spots has been observed. The motion is both in clockwise and counter-clockwise directions, in the same spot. The present observations do not fully confirm the existence or otherwise of the tangential velocities in sunspot penumbrae. However, in the light of the recent measures of the azimuthal component of magnetic field in sunspots by Adam, the presence of the tangential velocities could be expected.

A photometric analysis of the asymmetry in lines in the penumbral region has been presented. The direction of asymmetry in lines is always directed towards the general Evershed flow and seems to end near the outer penumbral boundary, while the Evershed flow continues in the photospheric region. The magnitude of the asymmetry in lines is a function of the line strength and the location in the spot region. The stronger lines show small asymmetry compared to the weaker lines. Near the disc centre positions of the spots, the asymmetry in general decreases. It is suggested that the phenomenon of line asymmetry may be due to the relative Doppler displacements occurring in several strata of the line forming layer, superimposed on small scale motion within the layer.

In the photospheric region of the spectrum, lines show slight "flaring". This is conspicuous in the darker portions of the spectrum. In the bright regions, due to the solar granules, lines appear very symmetrical and no "flaring" in lines is seen.

Introduction:—J. Evershed (1909a), while analysing sunspot spectra obtained at the Kodaikanal Observatory, noticed motion of sunspot gases in the penumbral region. The spectra clearly revealed a horizontal and radial outflow of gases in the penumbra. Further studies of Evershed (1909a, b, c, 1910, 1916) showed that the magnitude of the radial motion depends on the disc position of the spot and the strength of lines. Evershed's early observations of the radial motion in sunspots were later confirmed by the observations of St. John (1913). This discovery of radial horizontal flow of material in sunspot penumbrae, is now known as the Evershed Effect.

Much later Abetti (1932) observed 26 spots and reported that radial and tangential velocities vary from spot to spot. Abetti also showed that the radial velocity is a function of the spot area. Calamai (1934) suggested that the motion of gases in sunspots is of a logarithmic spiral type. During recent years, Kinman (1952, 1953), Bumba (1960), Holmes (1961), Servajean (1961) and Brekke and Per Maltby (1963) have extended the study of the Evershed Effect in sunspots. A detailed and precise knowledge of the velocity and magnetic fields in sunspots is essential for an understanding of the sunspot phenomenon.

For a precise understanding of the velocity fields in spots, it is necessary to have a large spectrographic dispersion, large image resolution and good seeing conditions. As suggested by Kinman (1953) the sight-line velocities in sunspots are affected by:

(1) the horizontal apparatus function of the spectrograph,

(2) The Zeeman broadening,

(3) obliteration of solar image due to the telescope, spectrograph and atmospheric conditions, and

(4) scattered light in the telescope and spectrograph.

To obtain an accurate velocity field configuration, it is necessary to minimise the above-mentioned obliterating effects. In the present study of the Evershed Effect, an image scale of 5.5″ per mm and a spectrographic dispersion of approximately 6 to 8 mm per Angstrom were utilized. Table I, contains the details of dispersion, velocity factors, image scale, number of spots studied and exposure times used in the Evershed Effect studies. To completely avoid the influence of the magnetic field from the velocity field determinations, three Zeeman-insensitive lines were selected. These lines; 4912.027 NiI, 5576.101 FeI and 5691.509 FeI (Ni), cover a limited range in excitation potential and in Rowland intensity. The details of the lines are given in Table II.

TABLE I

Details of Instrumentation used in the study of the Evershed Effect

Author	Year	Dispersion Å/mm	Doppler shift mm/km/sec	Image scale Sec. of arc/mm.	No. of Spots	Exposure Time seconds	Wavelength Region Å
Evershed	1909	1.1	0.014	16.3	12	30	4650
	1909	1.1	0.014	16.3	4	30	4650
	1916	1.1	0.014	22.0	2	5—30	4650
St. John	1919	0.56	0.025	11.0	11	60—180	
Abetti	1932	1.2	0.019	11.0	26	..	4000
Calamai	1934	1.5	0.013	11.0	5	..	..
Kinman	1952	1.5	0.019	10.8	1	5-6	5000
	1953	1.5	0.013	10.4	4	2—5	5900
Bumba	1960	0.29	0.068	5.9	22	1-2	5900
Servajean	1961	0.5	0.02	9.0	1	1—12	5000
Holmes	1961	0 17	0.109	5.8	1	30—60	5576
	1963	0.20	0.092	10.3	1	40—60	5576
Brekke and Per Maltby	1963	0.29	0.069	6.8	..	0.8—3	4754
Bhatnagar	1964	0.12	0.187	5.5	2	10—12	4912
		0.17	0.109	5.5	2	3	5576
		0.16	0.113	5.5	2	3	5691

TABLE 2

Details of Zeeman-Insensitive lines used for the velocity field determination

Wavelength Å	Element	Rowland Intensity		E.P. in volts		Transition
		Disc	Spot	Low	High	
4912.027	NII	1	1	9.75	6.26	$z^4F—e^4F$
5576.101	FeI	4	4	3.42	5.63	$z^5F—e^5D$
5691.509*	FeI	2	2	4.28	6.45	$y^5F—g^5D$

The observed sight-line velocity fields reveal only the sight-line velocity variation in the spots. These measures are insufficient to present a complete velocity field distribution in spots, unless the true direction of the mass motion in spots is known. Further, the knowledge of depth dependence of the mass motion is essential for a velocity field model of sunspots. Methods are available for resolving the observed sight-line velocities into three component velocities; radial, tangential and vertical. With a suitable model of the sunspot penumbra and using the theory of line formation, it is now possible to determine the depth dependence of velocity fields in sunspot penumbrae.

In this study the observed sight-line velocities in sunspot penumbrae, were resolved into three component velocities radial, tangential and vertical. The sunspot penumbra model of Makita (1963) was utilized for determining the mean depth of formation of lines. The spatial distribution of the longitudinal component of the spot magnetic field, was also determined for a study of a possible correlation between the velocity and the magnetic field configuration.

The observations.— The Kodaikanal solar tower telescope was utilized in this study. Light from a 60 cm aperture coelostat of fused quartz, was fed to a 38 cm aperture achromat of focal length 36.6 metres. A solar image of diameter 34.8 cms was formed on the spectrograph slit.

The 18 metre Littrow spectrograph in conjunction with the solar telescope, uses a grating ruled by Babcok as the dispersing unit. This grating of 600 grooves per mm is blazed in the fifth order green and has a ruled surface of 200×135 mm. Tests performed with an Iodine absorption tube have shown that close Iodine doublets at 5303 Å, having approximately 0.009 A separation are easily resolved in the fifth order. This shows that the theoretical resolving power of 600,000 of the grating is achieved.

To estimate the scattered light in the spectrograph, spectra were taken with different slit heights varying from 0.5 cm to 2.5 cms. Long exposures were given to greatly over expose the spectra. No blackening beyond the spectrum edges on these exposures were perceptible. Photoelectric determinations have also shown no perceptible contribution due to diffuse scattered light in the spectrograph. We have, therefore, assumed that the effect of the scatterd light in the spectrograph on the observed velocities is negligible.

To determine the spatial variation of velocity and magnetic fields in sunspots five to six spectra were obtained with the slit of the spectrograph crossing various portions of the spot. To determine precisely the coordinates of the points where the Doppler displacements were measured on the spectrograms, two wires 300 microns thick were stretched over the slit jaws. These wires cast shadows on the spectrum

* This line is identified as blend of Fe (Ni) in the Rowland table.

which serve as fiducial marks on the plate. The spot spectra were taken after bringing the desired portion of the spot between these two wires. A recording of the position of the wires, the slit position and the spot, was made immediately after each exposure. The heliographic coordinates of the points, at which the velocity measurements were made, were determined by using these sunspot maps and the white light photoheliograms taken daily at Kodaikanal, around the time of four observations.

Measurement of Doppler shifts.—The Fraunhofer lines become very broad and diffuse under high dispersion, such as the one used in this study. However, it is essential to have high dispersion for a precise determination of small Doppler displacements. In the case of wide diffuse lines it becomes very difficult, if not impossible, to use the conventional method of measuring line positions bisecting the spectral line with a micrometer crosswire. The method used in this study, for measuring the sight-line velocities, utilizes essentially the principle of photographic subtraction. The principle was first used for wavelength determinations by Evershed (1913). The present method is, however, an extension of the original Evershed's positive-on-negative method, and is capable of yielding greater precision and convenience of measurement. The essential advantage of this method is that, the accuracy of the setting is independent of the width of lines. A more or less similar technique for measuring small Doppler shift was also used by Servajean (1961).

The spectrum to be measured was mounted on the plate carriage of a Zeiss spectrum projector, and was magnified 21 times. The projector yields a distortion-free enlargement. On the magnified images of the spectra, the scale and velocity factors in the three spectral regions of interest were as follows:

Wavelength Å	Scale Å/mm.	Velocity factor km/sec/mm.
4912	0.0060	0.360
5576	0.0060	0.426
5691	0.0078	0.415

The enlarged image of the line of interest in the spectrum was focussed on a stage attached to a micrometer screw. On this stage was mounted a suitable density positive enlarged copy of the line to be measured. Care was taken to see that the magnification of the positive copy and the enlarged image of the spectrum was exactly the same. For setting on the line centre, the stage on which the positive enlargement of the line was mounted, was moved to obtain a 'grey' match. At this position of the micrometer screw the positive profile precisely matches the negative. With a little practice it was possible to obtain a match within 50 to 60 microns of the micrometer scale, thus giving an accuracy of velocity measures of about 30 meters per second. A velocity measure obtained on the plate, is the mean velocity over 1.6 seconds of arc over the solar disk.

The plate carriage of the spectrum projector is capable of moving in two perpendicular directions : one along the dispersion, the X-direction, and the other perpendicular to it, the Y-direction. A precision dial gauge was attached in the Y-direction to read the position of the measured point from the wire shadow on the plate. The velocity measures were made at intervals of approximatey 1,100 km and on some plates at intervals of 1,900 km.

To determine the sight-line velocities in the sunspot, with respect to the velocity of a remote photospheric region, the following procedure was adopted. Line position settings on the two sides of spot were obtained using the 'grey' match technique. These

line positions were fitted into a straight line equation. Any deviation in the region of the spot, thus directly gives the sight-line displacement, due to the velocity field in the spot. This method enables one to smooth out small scale Dopper displacements due to the granular motion in the photospheric region.

This modified method of positive-on-negative, seems to be free from personal bias. However, matching becomes difficult when the line acquires an asymmetric profile, especially near the penumbral boundary.

From the formulae given by Walker (1909) or Minkowski (1942) for the curvature of lines in grating spectrograph, the maximum deviation in wavelength over a slight height of 14 mm, for a 60-foot spectrograph and in the wavelength region of interest is, less than 0.7 mA. The solar differential rotation on two sides of the spot observed was per sec. Considering their small magnitude, both these corrections to the velocity measures have been neglected.

Details of the sunspots studies and sight-line velocity field.— The observations reported in this study were obtained during two successive passages of the same sunspot group. This investigation was aimed to study the changes in velocity field with the age of the spot. The Kodaikanal photoheliogram records show that Kodaikanal spot No. 12358 (KKL 12358), first appeared around December 18, 1962, at about 14° east of the central meridian, and receded beyond the western limb on December 25. The same spot group appeared around January 8, 1963 on the eastern limb and was designated as KKL 12368. Until January 13, no apparent change in the shape and size could be noticed in the spot group. Between January 9 and 14 only two small flares were reported. From January 14 onwards rapid changes in shape and size were observed until January 18. During this interval, more than 7 sub-flares were reported in the CRPL data. It appears that from January 19 onwards, the spot group KKL 12368 attained the stable phase of its life. During its second passage across the disc, sight-line velocities were determined on January 13, 19, 20 and 21. The observed sight-line velocity fields are given in Figure 1 which shows variations in velocity fields between the pre-development and post-development phases of the sunspot.

The same spot group again appeared on the eastern limb on February 3, and is designated in Kodaikanal records as KKL 12375 on its third passage. The observations of the spatial velocity and magnetic fields were made on February 9, 10, 11, 12, 14, 15 and 16. Sight-line velocity fields are given in Figure 1. On February 9, the umbra of this spot (KKL 12375) appeared split into two, surrounded by a common penumbra. This appearance of the spot remained till February 11, and around February 12 ($L-L_o=0$) the two umbrae coalesced to form a single umbra. From the magnetic field plates and the shape of the spot, it was evident that the centre of the whole umbra was representative of the spot's centre.

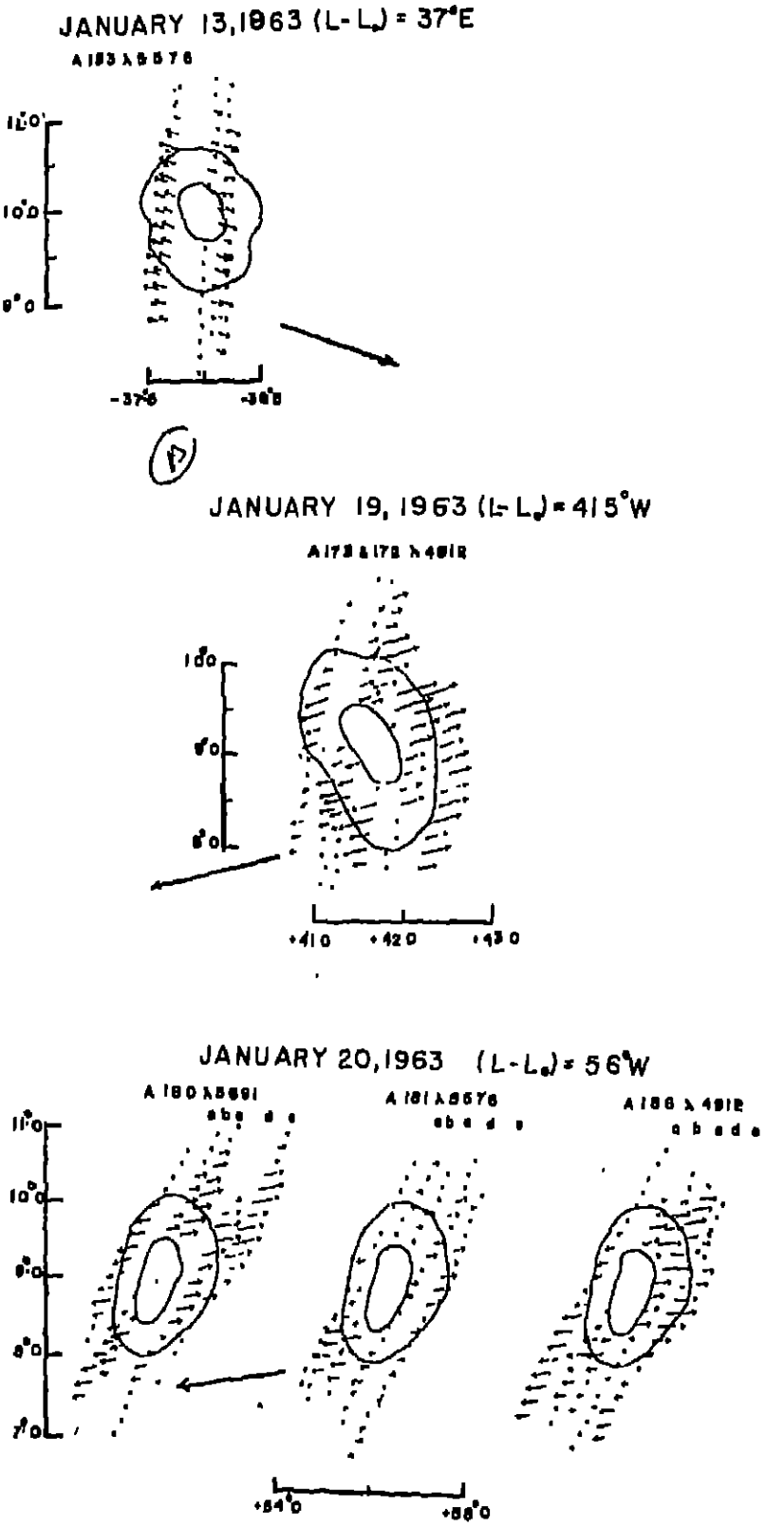

Figure 1 (a).—Sight line velocity field in Sunspots. Length of arrows are proportional to the magnitude of sight line velocity and the bold arrow indicates the approximate direction of the disc centre.

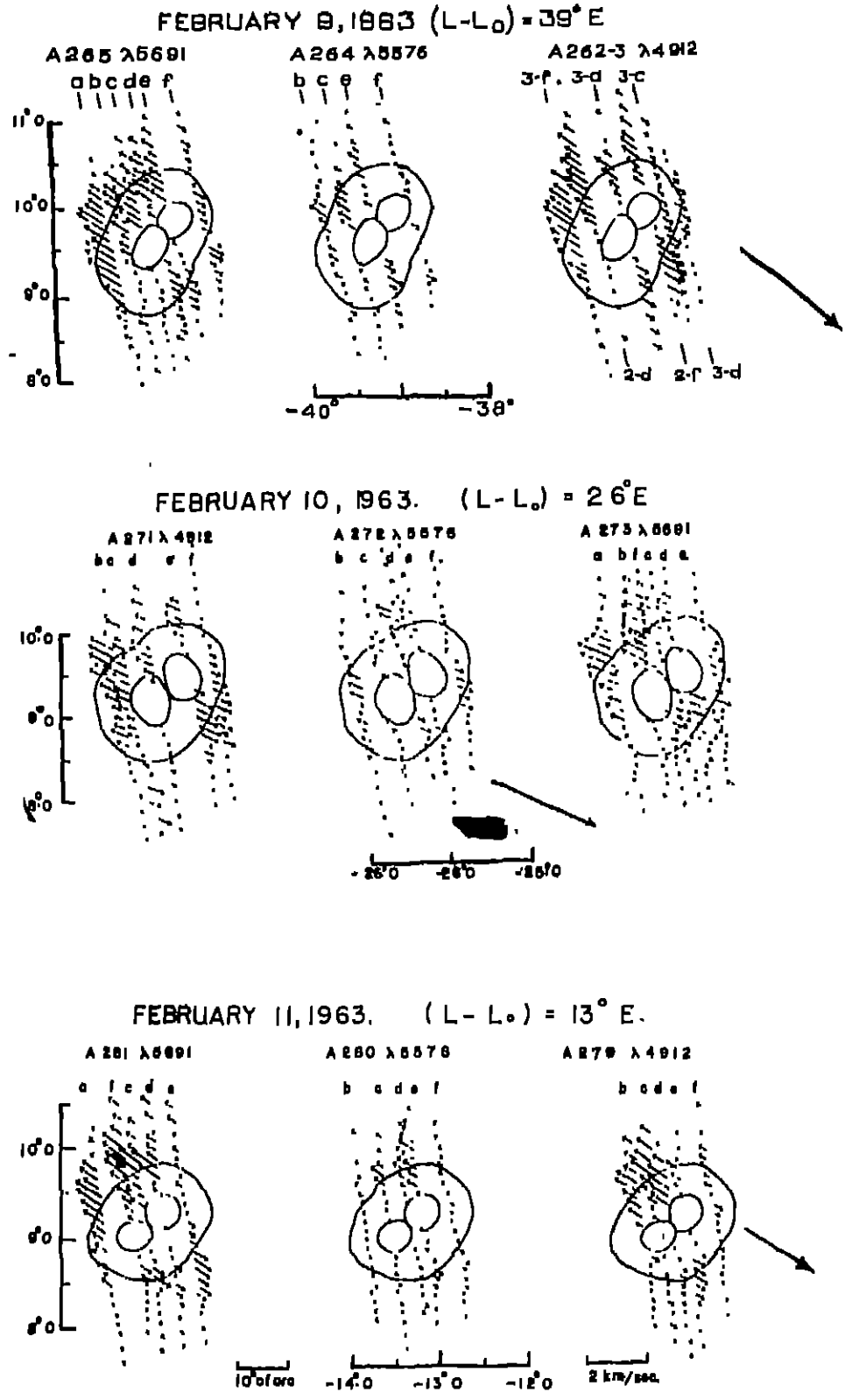

Figure 1 (b).—Sight line velocity field in Sunspots. Length of arrows are proportional to the magnitude of sight line velocity as and the bold arrow indicates the approximate direction of the disc centre.

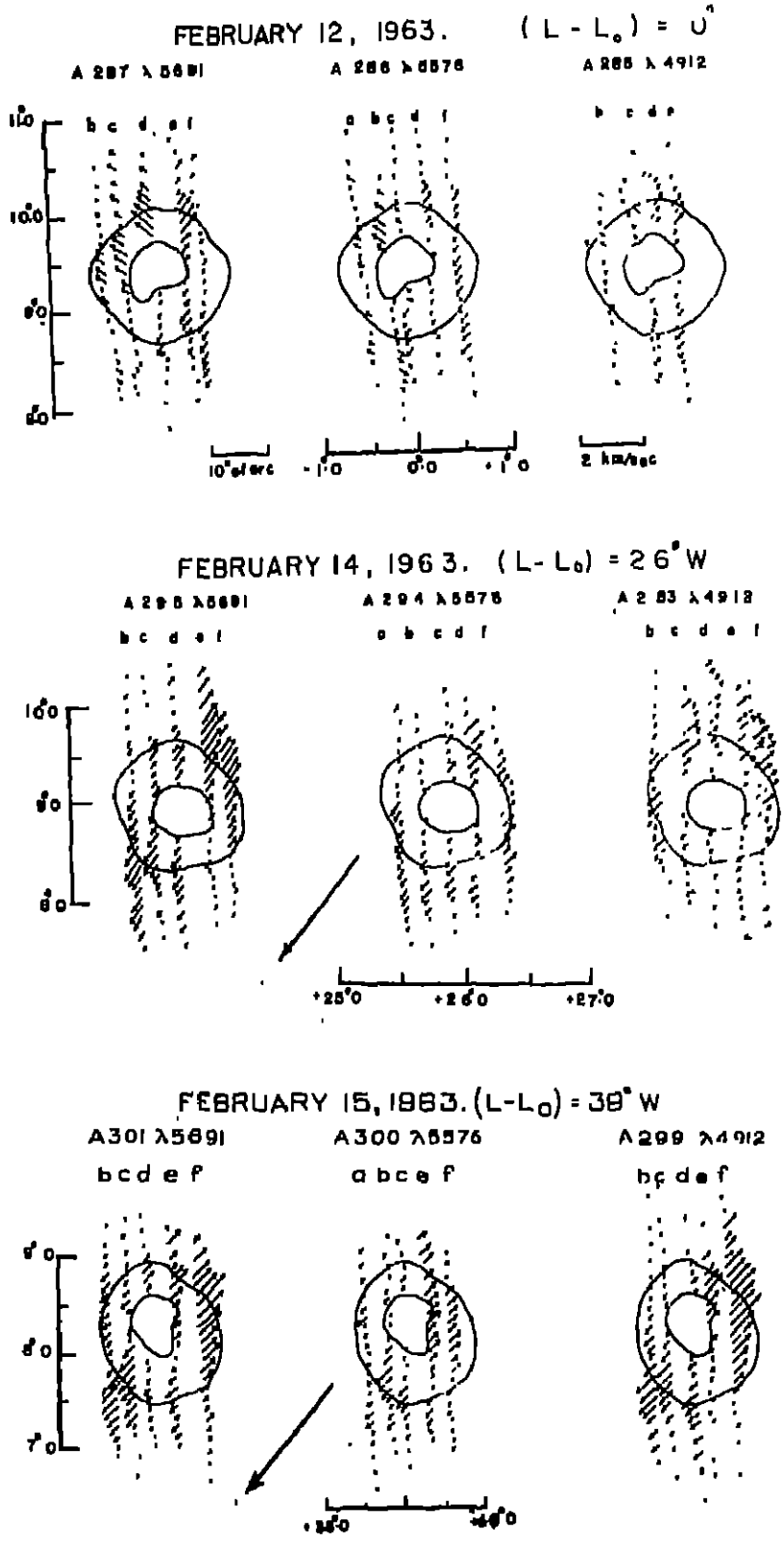

Figure 1 (c).—Sight line velocity field in Sunspots. Length of arrows are proportional to the magnitude of sight line velocity and the bold arrow indicates the approximate direction of the disc centre

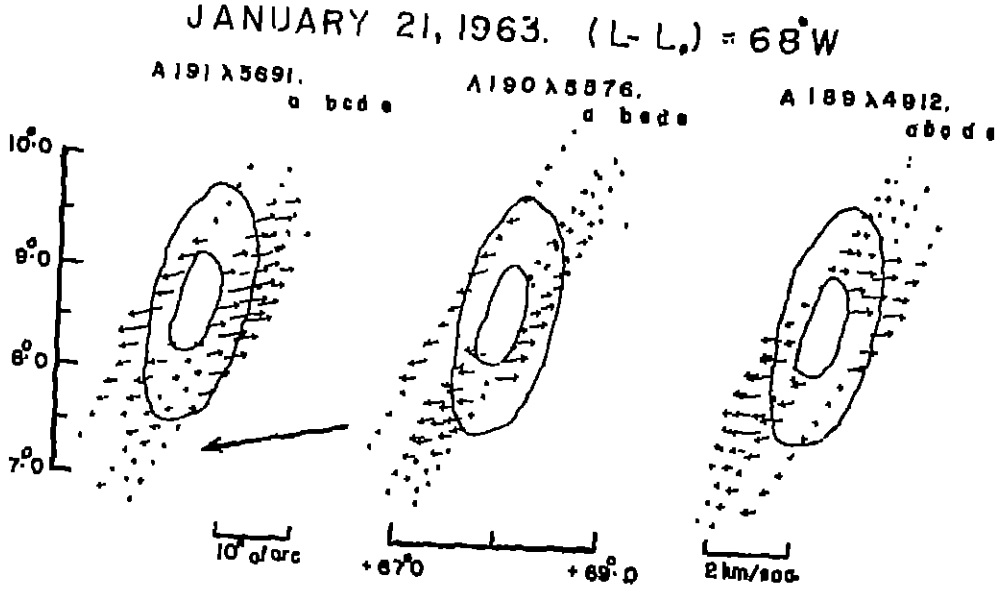

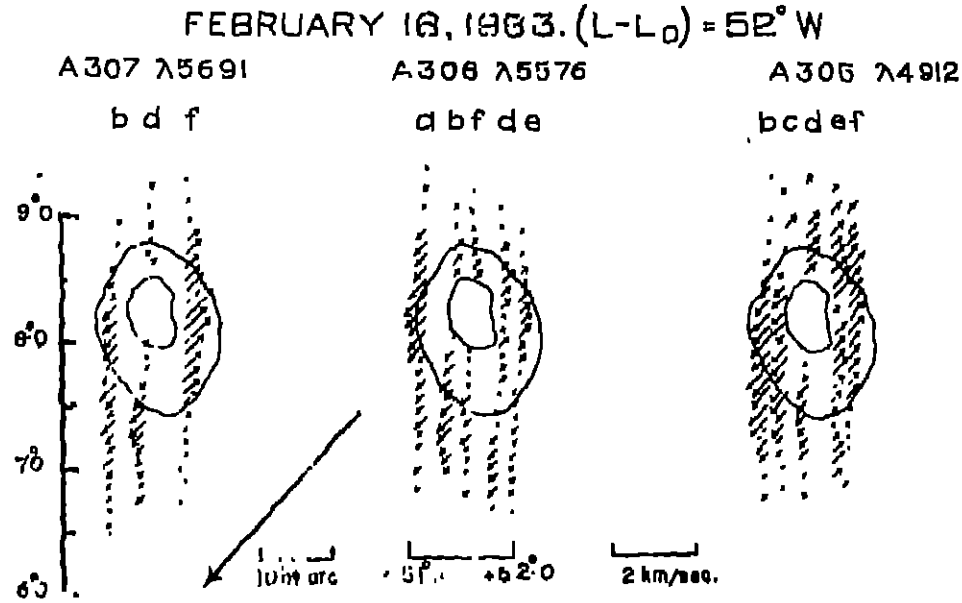

Figure 1 (d).—Sight line velocity field in Sunspots. Length of arrows are proportional to the magnitude of sight line velocity and the bold arrow indicates the approximate direction of the disc centre.

JAN. 19, A178 &9.

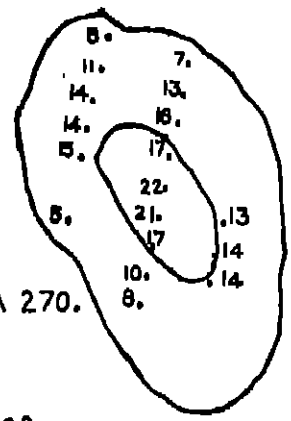

FEB.9, A 269.

FEB.10, A 270.

FEB.11, A 283.

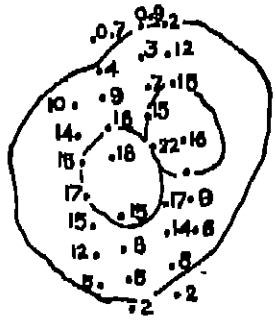

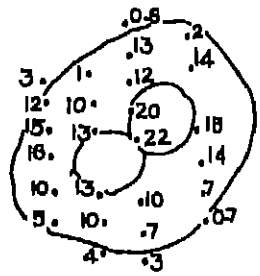

FEB.12, A 284.

FEB.14, A 286.

FEB.15, A 298.

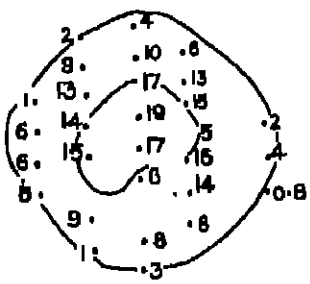

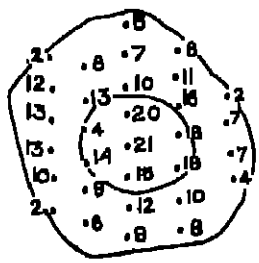

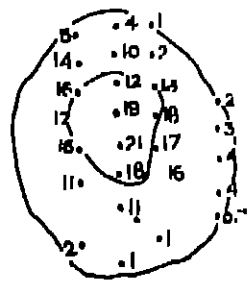

10.0

Figure 1.—Magnetic field in sunspots in units of 100 gauss.

The sunspot KKL 12375 disappeared beyond the western limb around February 19, and reappeared on March 3, on the eastern limb, with more or less the same shape that it had on the previous passage. Since March 5, until the spot vanished on the disc around March 14, 10 sub-flares of importance 1 to 1^- were reported. From the flare data and the configuration of the sunspot group, it is definite that from January 19 through March 3, this spot was in a stable and well developed phase of its life.

The variation of the velocity field configuration during the two passages and at the same disc position is an indication of the change in the velocity with the age of the spot.

Spatial magnetic field in sunspots: The spatial distribution of magnetic field was determined for those spots for which velocity fields were obtained. The aim was to detect any inhomogeneity in the magnetic field greater than 100 gauss, that would affect the velocity field distribution.

The observations were made using a compound quarter wave plate and a polaroid mounted in front of the slit of the spectrograph. The Zeeman sensitive line, 6303 A was used for these measurements. The polarity of the observed spot was tied in with the visual measures of the same spot obtained at the Mt. Wilson Observatory.*

The spot's magnetic field, measured on seven days (January 19, February 9, 10, 11, 12, 14 and 15), shows a positive polarity indicating that the magnetic lines of force are directed outwards from the solar surface. The spatial magnetic field distribution for each day is given in Figure 2. The number against each point on these sunspot maps represents the magnetic field strength in units of hundred gauss.

* I am thankful to Dr. R. Howard for kindly supplying the sunspot maps giving the magnetic field strength and polarity of some sunspots for comparison purposes.

Determination of Component Velocities in sunspot penumbrae: The sight-line velocity that we measure on a spot spectrum, is the velocity of the line-forming layers along the line of sight. For an understanding of the physical processes of motion in sunspots, it is essential to have a knowledge of the mode of flow of material in sunspots, independent of the line of sight.

In order to reduce the measured sight-line velocities to the component velocities (radial, tangential and vertical) in the spot, it is convenient to assume a polar coordinate system $(r, \varnothing)$ with the centre of the umbra (B, L) as origin. The distance from the spot centre, r, and the position angle, $\varnothing$ (measured from west through north) of any point (neglecting the curvature of the solar surface around the spot) are given by :

$$r = R_o \left[(\Delta\lambda \cos B)^2 + (\Delta B)^2 \right]^{\frac{1}{2}} \quad \text{and}$$

$$\tan \phi = \frac{\Delta B}{\Delta\lambda \cos B}$$

where R_o is the radius of the Sun, and ΔB and $\Delta\lambda$ are the differential heliographic coordinates of the point measured from the centre of the sunspot.

The three components of the sight-line velocity, which would completely define the velocity fields in a spot are the radial velocity u, component directed radially away from the spot centre, the tangential velocity v, directed normal to the radius vector of the spot and the vertical velocity w, directed perpendicular to the solar surface. It is convenient to use the cylindrical coordinate system to obtain the three component velocities in spots. The radial, tangential and vertical velocity components are given by

$$u = r, \quad v = r\phi \quad \text{and} \quad w = z$$

The corrected sight-line velocity is given by (Plaskett 1952)

$$V = u(\cos\phi \cos\gamma_1 + \sin\phi \cos\gamma_2) + V(\cos\phi \cos\gamma_2 - \sin\phi \cos\gamma_1) + w\cos\gamma_3 \quad \ldots\ldots\ldots\ldots\ldots\ldots (1)$$

where $\cos\gamma_1$, $\cos\gamma_2$ and $\cos\gamma_3$ are the direction cosines of the line of sight that depend on the position of the measured point and which are given by

$$\cos\gamma_1 = \sin(L-L_o)\cos B_o \sin(\theta+\theta_1)\operatorname{cosec}\theta$$
$$\cos\gamma_2 = [\sin B \cos B_o \cos(L-L_o) - \cos B \sin B_o] \sin(\theta+\theta_1)\operatorname{cosec}\theta$$
$$\cos\gamma_3 = -\cos(\theta+\theta_1)$$

For the spots observed, the value of θ_1 does not exceed 0.1^0 and is neglected. The heliocentric distance $(L-L_o)$, and the heliographic latitude B for any measured point on the solar disc were obtained from the sunspot maps. B_o and L_o are given for each day in the Nautical Almanac.

Equation (1) involves three unknown quantities u, v, and w. To determine these unknowns, three equations of the type (1) are required. Following Kinman (1952, 1953), it was assumed that the motion has a cylindrical symmetry about the spot's centre and that all points equidistant from the centre of the spot, satisfy the equation of condition (1). The measured points around the spot were divided into annular zones of width 750 km to 1000 km, and for each annular zone we have the following equations,

$$\left.\begin{aligned} V_1 &= uX_1 + vY_1 + wZ_1 \\ V_2 &= uX_2 + vY_2 + wZ_2 \\ \ldots &\quad \ldots \quad \ldots \quad \ldots \\ V_n &= uX_n + vY_n + wZ_n \end{aligned}\right\} \quad \ldots\ldots\ldots\ldots\ldots\ldots\ldots\ldots\ldots\ldots (2)$$

where

$$X = (\cos\phi \cos\gamma_1 + \sin\phi \cos\gamma_2)$$
$$Y = (\cos\phi \cos\gamma_2 - \sin 0 \cos\gamma_1)$$
$$Z = \cos\gamma_3 = -\cos 0$$

In the polar coordinate system (r, Φ) with the spot centre as the origin, it is assumed that the spot surface is plane. In equation (1) the coefficient of w, $\cos\gamma_3$ (=cos 0) is independent of ∅ and is assumed constant over the spot surface. Following Servajean (1961), we have made $\cos\gamma_3$ constant and the vertical velocity component w in the spot, is referred with respect to a distant point in the photosphere.

An IBM 1620 computer was used to obtain the component velocities u, v and w from the solution of equations (2) for each annular zone. In the same programme instructions were coded to yield data required for the root square errors of u, v and w velocities. The component velocities u, v and w, were obtained for each of the three lines as measured on the spectra obtained on January 20 and 21 and February 9, 10, 11, 12, 14, 15 and 16.

Determination of mean depths of formation of lines: An absorption line in the solar spectrum is formed over a considerable thickness of the solar atmosphere. Individual strata contribute to the formation of a line, depending on the physical parameters of each layer. A knowledge of the model of the atmosphere, that is, the dependence of temperature, pressure and the continuous absorption coefficient on depth is essential for determining the mean depth of formation of a line. With the availability of a sunspot penumbra model given by Makita (1963), it was possible to determine the mean depth of formation of lines in the penumbral region.

The residual intensity of a point on the line profile is defined by

$$r_\lambda = \frac{I_{\lambda_0}(O, \mu) - I_{\Delta\lambda}(o, \mu)}{I_{\lambda_0}(o, \mu)} \qquad \ldots\ldots(3)$$

Writing in the form indicated by Pecker (1951) and making use of the weighting function, $v_{i\lambda}$ is given by the equation

$$r_\lambda = \int_o^\infty G\Psi\left(\frac{k\Delta\lambda}{k\lambda_0}\right)\frac{d\tau}{\mu} \qquad \ldots\ldots(4)$$

where the weighting function G, is given by

$$G = \frac{\int_\tau^\infty B(\tau)\left[\exp-\left(\frac{\tau}{\mu}\right)\right]\frac{d\tau}{\mu} - B(\tau)\left[\exp-\left(\frac{\tau}{\mu}\right)\right]}{\int_o^\infty B(\tau)\left[\exp-\left(\frac{\tau}{\mu}\right)\right]\frac{d\tau}{\mu}} \qquad \ldots\ldots(5)$$

and Ψ, the saturation function

$$\Psi = \exp\left\{-\int_o^\tau\left(\frac{k_{\Delta\lambda}}{k_{\lambda_0}}\right)\frac{d\tau}{\mu}\right\} \qquad \ldots\ldots(6)$$

where B (τ)=Planck function,

μ=cos θ, θ being the angle between the solar radius at the point of observation on the disc and the line of sight,

$k\lambda_0$=continuous absorption coefficient per hydrogen atom,

$k\Delta\lambda$=selective absorption coefficient per hydrogen atom.

In equation (5) the source function is made equal to the Planck function at an optical depth τ. The source function is given by the expression,

$$B(\tau) = a + b\tau + c\,E_2(\tau) \qquad \ldots\ldots(7)$$

where $E_2(\tau)$ is the exponential integral, and a, b, and c are the limb darkening constants.

Integrating (7) and using the property of exponential integrals and substituting in (5), it can easily be shown that

$$G = \frac{\mu \exp\left[-\frac{\tau}{\mu}\left\{b + c\left[E_1\left(\frac{\tau}{\mu}+\tau\right) - E_1(\tau)\right]\right\}\right]}{a + b\mu + c\left[1 - \mu \ln\left(1+\frac{1}{\mu}\right)\right]} \qquad \ldots\ldots(8)$$

To determine the weighting function G, at five disc positions, use of the solar limb darkening observations at 5000 A, of Pierce and Waddell (1961) was made.

Following ten Bruggencate *et al.* (1955), integration of equation (4) was carried over the log t scale and equation (4) takes the form

$$r_\lambda = \int_{-\infty}^{\infty} \frac{G}{\mu}\left(\frac{k_{\Delta\lambda}}{k\lambda_0}\right)\tau \cdot \frac{\Psi}{Mod}\, d(\log\tau) \qquad \ldots\ldots(9)$$

where

$$\Psi = \exp\left[-\int_{-\infty}^{\infty}\left(\frac{k_{\Delta\lambda}}{k\lambda_0}\right)\frac{\tau}{\mu}\,\frac{1}{Mod}\, d(\log\tau)\right] \qquad \ldots\ldots(10)$$

The selective absorption coefficient $k_{\Delta\lambda}$ per hydrogen atom is given by

$$k_{\Delta\lambda} = \frac{\sqrt{\pi}e^2\lambda_0^2}{mc^2} A.f.\,\frac{N_{la}}{N_a}\,\frac{1}{\Delta\lambda_D}\exp\left[-\left(\frac{\Delta\lambda}{\Delta\lambda_D}\right)\right] \qquad \ldots\ldots(11)$$

Assumption is made that the velocity measures refer only to the core of the line, where $\Delta\lambda$=0, A is the number of atoms of the element per hydrogen atom, f is the oscillator strength, N is the number of atoms of the element in the energy level corresponding to the transition responsible for the line, N_a is the total number of atoms of that element, and $\Delta\lambda_D$ is the Doppler width, given by

$$\Delta\lambda_D = \frac{\lambda}{C}\sqrt{\frac{2RT}{M} + \xi^2 t_n} \qquad \ldots\ldots(12)$$

$\sqrt{\frac{2RT}{M}}$ gives the thermal velocity and ξt_n, the turbulent velocity, was neglected because of its unknown contribution in the calculation of the Doppler width of lines. The quantity $\frac{(N_{la})}{(N_a)}$ in equation (11) was directly obtained from the combined Saha and Boltzmann equations, for each of the temperature and electron pressure values in the penumbra model.

The continuous absorption coefficient k_{λ_0} is given by

$$k_{\lambda_0} = \frac{N_{OII}}{N_H}\left(k_{\lambda_0} + k_{\lambda_0}^{-} P_e\right) \quad \ldots\ldots(13)$$

Contribution to the continuous absorption due to neutral hydrogen was neglected and only the contribution due to the negative hydrogen ion was considered.

The saturation function Ψ, was obtained by numerical integration of equation (10). The contribution curve is given by

$$\gamma = G\left[\frac{K}{\mu}\cdot\frac{\tau}{\Delta\lambda_D}\cdot\frac{N_{Ia}}{N_a}\cdot\frac{I}{k\lambda_0}\right]\Psi$$

where

$$k = \frac{\sqrt{\pi e^2}\lambda_0^2}{mc^2} A.f. \quad (14)$$

The abundance A, was obtained from Goldberg *et al.* (1961) and the oscillator strength f, of the lines from Wright's (1944) curve of growth.

Figure 3 shows the contribution curves for the line centre, for each of the two lines (4912 and 5691) at five disc positions. The bisector of the arae under each contribution curve gave the mean optical depth of formation of the line and thus determined the mean geometrical depths of formation of each of the two lines. The mean depth of formation of 5576.101 Å Fe I, of Rowland intensity 4, in the sunspot penumbra seems to lie much higher than the other two lines, used in this study. The Makita penumbra model at our disposal does not permit us to obtain a complete contribution curve for this line.

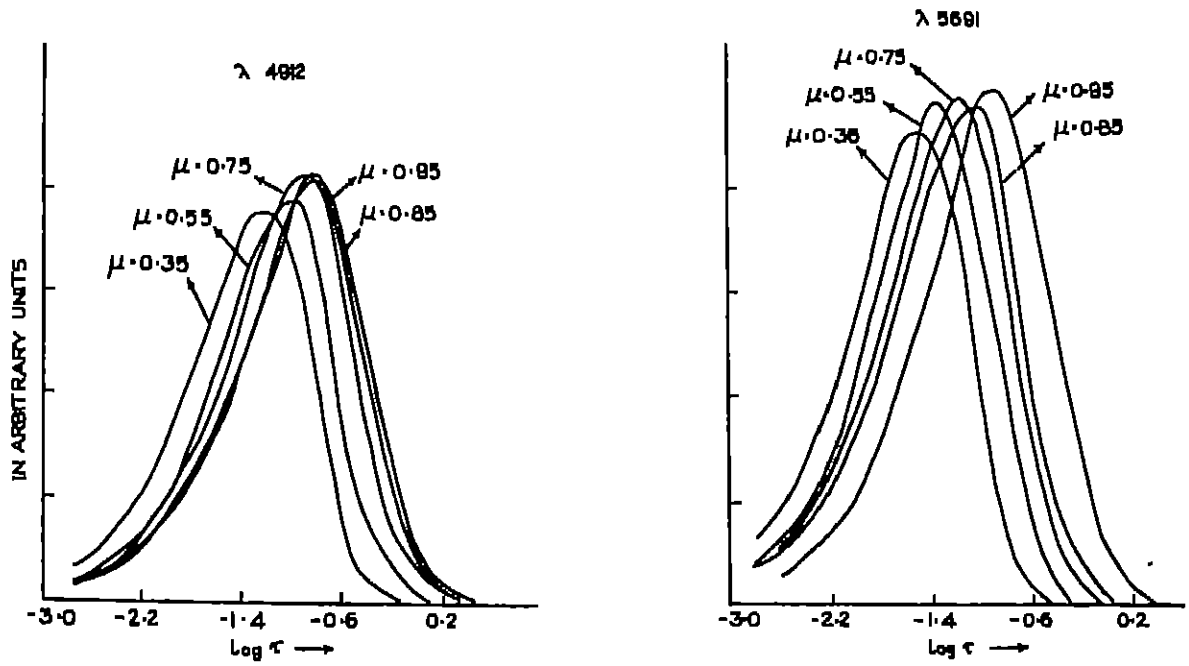

Figure 3.—Contribution curves for 4912 and 5961 in sunspot penumbra.

In Table 3 is given the mean depth of formation of lines 4912.027 Ni I Rowland intensity 1 and 5691.508 Fe I Rowland intensity 2 in the penumbral region.

TABLE 3

Mean optical and geometrical depth of formation of 4912 *and* 5691 *and the gradient of Umax with depth at nine disc positions of the spot*

Date	μ	Depth of formation of 4912 Ni I		Depth of formation of 5691 Fe I		Gradient of U_{max} in km/sec/km.
		log *t*	*z* km	log *t*	*z* km	
20 Jan.	0,55	—1.21	180	—1.42	145	9.1×10^{-5}
21 Jan.	0,35	—1.36	155	—1.62	117	4.5×10^{-4}
9 Feb.	0.75	—1.04	215	—1.20	166	1.6×10^{-5}
10 Feb.	0,85	—0.98	230	—1.24	175	0.9×10^{-5}
11 Feb.	0,95	—0.96	235	—1.16	168	1.3×10^{-5}
12 Feb.	0,95	—0.96	235	—1.16	168	6.2×10^{-5}
14 Feb.	0,85	—0.98	230	—1.24	175	7.2×10^{-5}
15 Feb.	0.75	—1.04	215	—1.29	166	3.8×10^{-5}
16 Feb.	0,55	—1.21	180	—1.42	149	2.3×10^{-4}

Discussion of the component velocities: (a) *The radial velocity field ;* The radial velocity component u, has the largest contribution to the mass motion in sunspot. The component velocity u, was determined using the three Zeeman insensitive lines, at two disc positions during the first passage and at seven disc positions during its second passage across the disc. Figure 4 gives the run of the component velocities u, and w and their r.m.s. errors obtained from each of the 3 lines and at 3 disc positions of the spot. At the top of each figure, the extent of the umbra and penumbra are represented by the dark and hatched regions respectively. Table 4 gives the magnitudes of radial, tangential and vertical velocities and their r.m.s. errors.

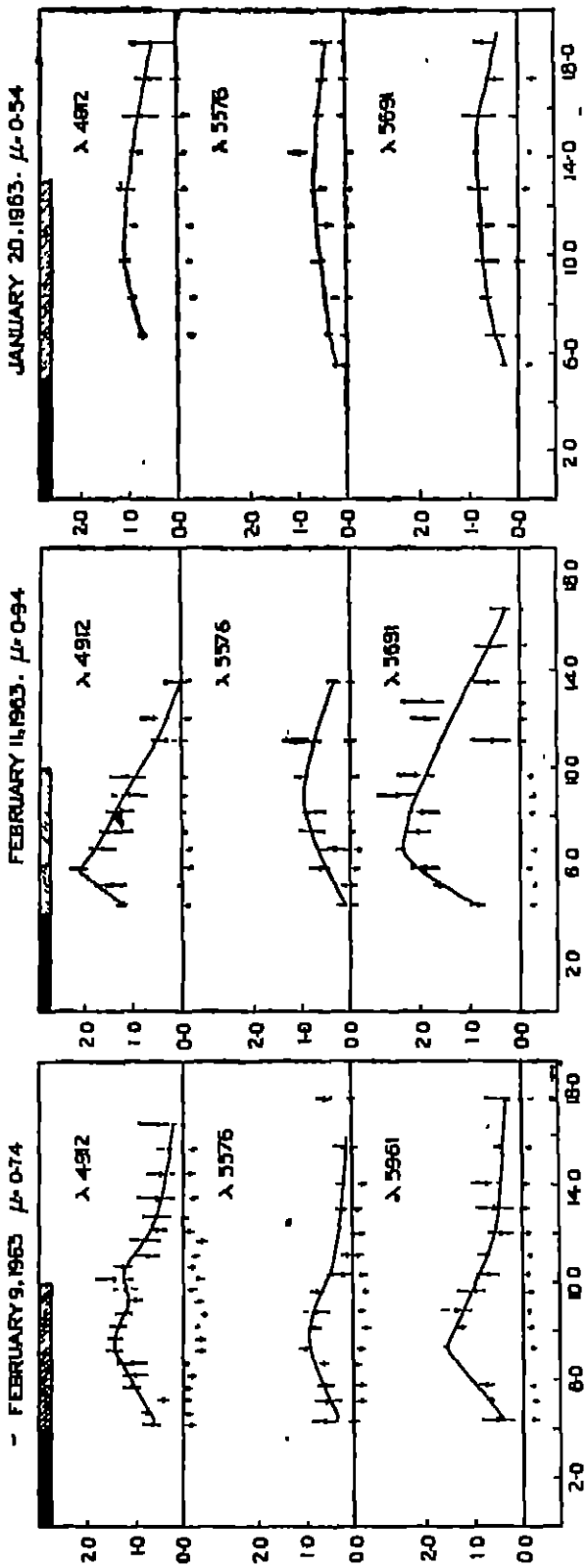

Figure 4—Run of radial and vertical velocities measured in three lines on three disc positions of the sunspot.
Ordinate — in units of km/sec.
Abscissa — in units of 1000 km.

TABLE 4

Component velocities in km/sec. in Sunspot No. KKL 12375 on February 9, 1963 at $\mu = 0{\cdot}74$

Spectral line used		Distance from the centre of the spot in 10^8 km.									
		4.25	4.75	5.25	5.75	6.25	6.75	7.25	7.75	8.25	8.75	9.25
4912 (A263)	u	+0.57	+0.02	+0.44	+1.14	+1.06	+1.13	+1.48	+1.46	+1.92	+1.24	+1.05
	r.m.s.	0.21	0.02	0.13	0.20	0.28	0.31	0.21	0.18	0.18	0.17	0.20
	v	+0.35	+0.07	−0.41	−0.06	+0.91	+0.56	−0.07	−0.31	−0.19	−0.60	−0.27
	r.m.s.	0.24	0.08	0.15	0.28	0.21	0.31	0.29	0.16	0.24	0.19	0.17
	W − W_0	−0.15	−0.07	−0.07	−0.06	−0.17	+0.01	−0.36	−0.33	−0.26	−0.40	−0.32
	r.m.s.	0.09	0.01	0.02	0.12	0.12	0.15	0.11	0.08	0.10	0.08	0.09

Spectral line used		Distance from the Centre of the spot in 10^8 km.									
		9.75	10.2	10.7	11.2	11.7	12.2	12.7	13.2	14.2	15.2	16.2
4912 (A263)	u	+1.57	+1.47	+1.80	+0.76	+0.18	+0.61	+0.60	+0.68	+0.51	+0.29	+0.64
	r.m.s.	0·28	0·42	0·21	0·20	0·32	0·25	0·33	0·43	0·22	0·30	0·40
	v	−0·96	−0·88	−0·34	+0·09	+0·05	−0·12	+0·18	−0·11	−0·09	+0·24	−0·11
	r.m.s.	0·26	0·35	0·15	0·20	0·20	0·17	0·30	0·28	0·16	0·27	0·29
	W − W_0	−0·12	−0·25	−0·15	−0·20	−0·34	−0·16	−0·02	−0·14	−0·11	−0·22	−0·00
	r.m.s.	0·13	0·18	0·06	0·13	0·13	0·08	0·08	0·14	0·06	0·11	0·10

TABLE 4—(*Contd.*)

Component velocities in km/sec. in Sunspot No. KKL 12375 *on February* 9, 1963 *at* $\mu = 0.74$

Spectral line used		Distance from the centre of the spot in 10^3 kms.						
		4·37	5·13	5·87	6·62	7·37	8·13	8·87
5576 (A264)	u	+0·67	+0·54	+0·58	+0·67	+1·02	+0·88	+0·77
	r.m.s.	0·26	0·30	0·21	0·07	0·12	0·17	0·28
	v	+0·08	+0·12	+0·27	—0·02	—0·21	—0·38	—0·12
	r.m.s.	0·23	0·18	0·22	0·07	0·10	0·16	0·16
	W—W_e	0·00	—0·16	—0·16	—0·06	—0·12	—0·24	—0·13
	r.m.s.	0·10	0·11	0·10	0·09	0·05	0·07	0·09
5691 (A265)	u	+0·53	+0·60	+0·76	..	+1·57	+1·24	+1·37
	r.m.s.	0·40	0·01	0·13	..	0·01	0·02	0·35
	v	+0·16	+0·37	+0·36	..	—0·06	—0·33	—0·25
	r.m.s.	0·24	0·05	0·13	..	0·06	0·00	0·08
	W—W_e	—0·22	—0·25	—0·20	..	—0·21	—0·14	—0·10
	r.m.s.	0·13	0·02	0·06	..	0·00	0·00	0·04

Spectral line used		Distance from the centre of the spot in 10^3 km.							
		9·62	10·3	11·1	12·0	13·0	14·0	15·5	17·5
5576 (A264)	u	+0·78	+0·24	+0·18	+0·07	+0·27	+0·25	+0·26	+0·60
	r.m.s.	0·14	0·35	0·14	0·18	0·20	0·21	0·20	0·20
	v	—0·15	+0·29	+0·37	+0·11	+0·38	—0·11	+0·19	—0·08
	r.m.s.	0·13	0·38	0·11	0·10	0·40	0·17	0·23	0·09
	W—W_e	—0·23	—0·14	—0·08	—0·15	—0·09	—0·21	0·00	0·00
	r.m.s.	0·05	0·12	0·04	0.04	0·11	0·06	0·08	0·02
5691 (A265)	u	+1·00	+0·71	+0·78	+0·49	+0·62	+0·78	+0·47	+0·30
	r.m.s.	0·43	0·23	0·15	0·30	0·42	0·30	0·17	0·58
	v	+0·01	—0·02	0·00	—0·33	—0·19	—0·38	—0·02	—0·32
	r.m.s.	0·25	0·18	0·13	0·19	0·18	0·20	0·11	0·19
	W—W_e	—0·14	—0·04	—0·12	—0·11	—0·03	+0·06	—0·15	0·00
	r.m.s.	0·14	0·09	0·05	0·10	0·11	0·09	0·04	0·06

TABLE 4—(*Contd.*)

Component velocities in km/sec. in Sunspot No. KKL 12375 on February 10, 1963 at $\mu = 0.86$

Spectral line used		Distance from the centre of the spot in 10^4 km.						
		4·37	5·13	5·87	6·21	7·37	8·13	8·87
4912 (A271)	u	+1·09	+1·54	+1·73	+1·64	+1·47	+1·20	+1·37
	r.m.s.	0·31	0·35	0·10	0·10	0·04	0·17	0·17
	v	+0·23	−0·15	−0·07	−0·16	−0·26	−0·36	−0·10
	r.m.s.	0·36	0·36	0·10	0·11	0·04	0·20	0·18
	W—W_o	−0·29	−0·06	+0·01	−0·09	−0·07	−0·01	−0·12
	r.m.s.	0·12	0·12	0·03	0·03	0·01	0·07	0·06
5576 (A272)	u	+0·63	+0·79	+1·22	+1·08	+0·91	+1·02	+0·76
	r.m.s.	0·13	0·14	0·30	0·14	0·07	0·12	0·09
	v	−0·18	+0·05	−0·29	−0·25	+0·24	+0·12	+0·14
	r.m.s.	0·13	0·02	0·22	0·13	0·08	0·14	0·10
	W—W_o	−0·02	−0·18	−0·06	−0·05	0·08	0·09	−0·18
	r.m.s.	0·03	0·06	0·09	0·05	0·02	0·05	0·09
5691 (A273)	u	+1·56	..	..	+1·55	+1·83	+1·43	+1·31
	r.m.s.	0·41	..	..	0·25	0·31	0·24	0·22
	v	−0·09	..	..	+0·18	−0·19	−0·09	+0·13
	r.m.s.	0·20	..	..	0·20	0·25	0·22	0·24
	W—W_o	+0·20	..	..	+0·06	−0·05	−0·10	−0·15
	r.m.s.	0·12	..	..	0·10	0·09	0·09	0·07

Spectral line used		Distance from the centre of the spot in 10^4 km.						
		9·62	10·30	11·10	12·00	12·60	13·50	15·00	16·50
4912 (A271)	u	+1·36	+0·93	+1·38	+0·75	+0·74	+0·74	+0·11	.
	r.m.s.	0·22	0·44	0·23	0·56	0·44	0·31	0·52	..
	v	−0·28	+0·04	−0·15	+0·40	+0·24	−0·33	+0·31	..
	r.m.s.	0·24	0·28	0·40	0·31	0·37	0·25	0·37	..
	W—W_o	−0·09	−0·07	−0·15	+0·09	−0·10	+0·04	0·00	..
	r.m.s.	0·09	0·11	0·12	0·10	0·13	0·07	0·11	..
5576 (A272)	u	+0·80	+0·80	+0·87	+0·90	+0·46	+0·69	−0·31	..
	r.m.s.	0·28	0·00	0·77	0·11	0·37	0·35	0·25	..
	v	+0·01	−0·20	+0·09	−0·28	−0·01	−0·14	+0·20	..
	r.m.s.	0·23	0·07	0·50	0·08	0·28	0·28	0·30	..
	W—W_o	−0·18	−0·19	−0·28	−0·10	−0·19	−0·16	0·00	..
	r.m.s.	0·09	0·02	0·17	0·03	0·06	0·09	0·06	..
5691 (A273)	u	+1·43	+1·35	+0·92	+0·55	+0·70	..	+0·07	−0·11
	r.m.s.	0·35	0·25	0·30	0·30	0·24	..	0·38	0·25
	v	+0·21	−0·22	+0·29	−0·12	+0·31	..	−0·01	+0·17
	r.m.s.	0·38	0·20	0·25	0·24	0·23	..	0·20	0·23
	W—W_o	−0·21	−0·03	−0·12	−0·17	+0·01	..	−0·10	0·00
	r.m.s.	0·12	0·07	0·07	0·06	0·00	..	0·08	0·03

TABLE 4—(*Contd.*)

Component velocities in km/sec in Sunspot No. KKL 12375 on February 11, 1963 at $\mu = 0.94$

Spectral line used		Distance from the centre of the spot in 10^3 km.						
		4.37	5.13	5.87	6.62	7.37	8.13	8.87
4912 (A279)	u	+1.25	+1.71	+2.15	+1.82	+1.88	+1.25	+1.09
	r.m.s.	0.11	0.34	0.15	0.30	0.36	0.30	0.39
	v	−0.29	+1.11	−1.09	−0.19	−0.07	+0.08	+0.14
	r.m.s.	0.14	0.54	0.23	0.41	0.34	0.34	0.46
	W−W$_0$	−0.10	+0.07	−0.12	−0.16	+0.02	−0.01	−0.04
	r.m.s.	0.08	0.09	0.08	0.07	0.09	0.09	0.10
5576 (A280)	u	+0.18	+0.09	+0.63	+0.33	+0.81	+0.76	..
	r.m.s.	0.12	0.10	0.25	0.40	0.26	0.32	..
								..
	v	+0.28	+0.26	+0.40	+0.28	+.031	+0.40	..
	r.m.s.	0.14	0.10	0.33	0.30	0.30	0.37	..
	W W$_0$	−0.05	−0.04	−0.08	−0.18	−0.02	−0.01	..
	r.m.s.	0.03	0.02	0.07	0.09	0.07	0.08	..
5691 (A281)	u	+0.84	+1.69	+1.96	+2.42	+2.14	+2.01	+2.56
	r.m.s.	0.15	0.13	0.35	0.18	0.27	0.38	0.45
	v	+0.20	−0.31	0.37	0.27	+0.83	−0.27	−1.33
	r.m.s.	0.19	0.13	0.43	0.18	0.45	0.38	0.51
	W −W$_0$	−0.25	−0.27	−0.17	−0.30	−0.01	−0.25	−0.26
	r.m.s.	0.03	0.03	0.08	0.04	0.09	0.08	0.10

Spectral line used		Distance from the centre of the spot in 10^3 km.						
		9.62	11.10	12.00	12.60	13.50	15.00	17.50
4912 (A279)	u	+1.17	+0.31	+0.57	..	+0.07	..	..
	r.m.s.	0.35	0.32	0.30	..	0.30	..	..
	v	+0.06	+0.30	+0.24	..	+0.26	..	..
	r.m.s.	0.40	0.48	0.40	..	0.14	..	..
	W−W$_0$	−0.05	+0.02	−0.10	..	0.00	..	..
	r.m.s.	0.07	0.07	0.07	..	0.09	..	..
5576 (A280)	u	+1.11	+1.00	..	..	+0.35	..	..
	r.m.s.	0.15	0.47	..	..	0.15	..	..
	v	−0.97	−0.11	..	..	+0.30	..	..
	r.m.s.	0.27	0.64	..	..	0.20	..	..
	W−W$_0$	−0.04	−0.01	..	..	0.00	..	..
	r.m.s.	0.12	0.11	..	..	0.03	..	..
5691 (A281)	u	+2.15	+0.86	+1.98	+2.00	+0.68	+0.60	+0.80
	r.m.s.	0.39	0.41	0.30	0.47	0.26	0.36	0.32
	v	−0.78	0.00	−1.49	−1.95	−0.16	+0.28	−0.45
	r.m.s.	0.54	0.45	0.49	0.60	0.34	0.42	0.88
	W−W$_0$	−0.21	−0.01	−0.05	−0.04	0.00	0.00	−0.04
	r.m.s.	0.09	0.07	0.05	0.07	0.04	0.04	0.08

TABLE 4—(*Contd.*)

Component velocities in km/sec in Sunspot No. KKL 12375 on February 12, 1963 at $\mu = 0.95$

Spectral line used		Distance from the centre of the spot in 10^8 km.					
		4.37	5.12	5.87	6.62	7.37	8.13
4912 (A285)	u	+0.89	+1.13	+1.07	+1.27	+1.69	+1.53
	r.m.s.	0.06	0.21	0.39	0.55	0.54	0.48
	v	−0.50	−0.81	−1.33	−0.18	+0.02	−0.01
	r.m.s.	0.13	0.25	0.49	0.09	0.02	0.21
	W−W$_o$	−0.16	−0.02	−0.16	−0.16	−0.11	−0.13
	r.m.s.	0.01	0.01	0.00	0.19	0.18	0.10
5576 (A286)	u	+0.33	+0.93	+0.82	+0.97	+0.48	+0.88
	r.m.s.	0.19	0.41	0.22	0.24	0.24	0.21
	v	−0.64	−0.28	−0.11	−0.39	−1.06	−0.87
	r.m.s.	0.18	0.80	0.20	0.27	0.21	0.33
	W−W$_o$	−0.05	−0.11	−0.12	−0.10	+0.04	−0.10
	r.m.s.	0.02	0.15	0.01	0.05	0.05	0.05
5691 (A287)	u	+1.10	+1.09	..	+1.26	+1.59	+0.30
	r.m.s.	0.27	0.27	..	0.41	0.36	0.10
	v	−1.06	+1.77	..	−0.50	−1.06	−0.86
	r.m.s.	0.19	0.22	..	0.37	0.46	0.11
	W−W$_o$	−0.22	−0.34	..	−0.20	−0.21	+0.07
	r.m.s.	0.45	0.21	..	0.08	0.07	0.02

Spectral line used		Distance from the centre of the spot in 10^8 km.						
		8.05	9.62	10.50	11.50	13.00	15.00	16.09
4912 (A285)	u	+1.82	+1.19	+0.59	+0.96	..	+0.30	..
	r.m.s.	0.05	0.48	0.65	0.20	..	0.34	..
	v	−0.87	−0.89	−1.57	−1.89	..	+0.05	..
	r.m.s.	0.17	0.80	0.24	0.76	..	0.65	..
	W−W$_o$	−0.30	0.00	0.00	−0.11	..	0.00	..
	r.m.s.	0.16	0.11	0.16	0.10	..	0.03	..
5576 (A286)	u	+0.49	+0.68	+0.35	+0.71	+0.03	+0.39	..
	r.m.s.	0.28	0.39	0.48	0.43	0.25	0.24	..
	v	+0.91	−0.37	+0.39	−0.86	+0.01	−0.33	..
	r.m.s.	0.49	0.56	0.80	0.57	0.53	0.72	..
	W−W$_o$	−0.14	+0.12	+0.11	−0.09	+0.11	0.00	..
	r.m.s.	0.08	0.07	0.11	0.09	0.07	0.06	..
5691 (A287)	u	+1.14	+1.05	+0.98	+0.81	+0.53	+0.47	+0.26
	r.m.s.	0.88	0.22	0.19	0.39	0.33	0.15	0.16
	v	−0.79	−0.22	−1.43	−0.47	−0.64	−0.55	−0.37
	r.m.s.	0.59	0.33	0.30	0.25	0.92	0.45	0.52
	W−W$_o$	+0.01	0.00	−0.05	−0.10	−0.07	+0.04	0.00
	r.m.s.	0.08	0.05	0.04	0.17	0.08	0.05	0.03

TABLE 4—(*Contd.*)

Component velocities in km/sec in Sunspot No. KKL 12375 on February 14, 1963 at $\mu = 0.86$

Spectral line used		Distance from the centre of the spot in 10^8 km.						
		4.37	5.12	5.87	6.62	7.37	8.13	8.87
4912 (A295)	u	+0.81	+0.99	+1.47	+1.32	+1.19	..	+0.77
	r.m.s.	0.36	0.36	0.27	0.11	0.23	..	0.52
	v	−0.14	0.00	−0.07	−0.16	0.00	..	−0.06
	r.m.s.	0.30	0.35	0.26	0.29	0.25	..	0.35
	$W-W_0$	−0.02	−0.13	+0.02	−0.01	+0.01	..	+0.03
	r.m.s.	0.12	0.11	0.10	0.11	0.06	..	0.11
5576 (A294)	u	+0.78	+0.89	+0.79	+0.91	+0.91	+0.65	+0.62
	r.m.s.	0.11	0.09	0.13	0.27	0.40	0.36	0.28
	v	−0.03	+0.15	+0.31	−0.09	−0.11	+0.09	+0.30
	r.m.s.	0.10	0.11	0.11	0.25	0.37	0.19	0.56
	$W-W_0$	−0.37	0.36	−0.34	−0.38	−0.39	−0.29	−0.36
	r.m.s.	0.03	0.03	0.04	0.09	0.13	0.07	0.21
5691 (A295)	u	+1.19	+1.52	+1.70	+1.78	+1.80	+1.58	+1.21
	r.m.s.	0.09	0.12	0.11	0.20	0.24	0.40	0.75
	v	−0.30	−0.30	−0.15	−0.27	−0.19	+0.11	−0.28
	r.m.s.	0.09	0.12	0.09	0.17	0.16	0.24	0.47
	$W-W_0$	−0.16	−0.15	−0.10	−0.14	−0.09	+0.07	−0.14
	r.m.s.	0.03	0.04	0.03	0.06	0.06	0.09	0.15

Spectral line used		Distance from the centre of the spot in 10^8 km.						
		0.62	10.50	11.50	12.50	13.50	15.00	17.00
4912 (S293)	u	+1.06	+1.15	..	+1.25	..	+0.93	..
	r.m.s.	0.45	0.61	..	0.67	..	0.34	..
	v	+0.40	+0.63	..	0.00	..	+0.01	..
	r.m.s.	0.31	0.34	..	0.45	..	0.68	..
	$W-W_0$	+0.10	0.00	..	+0.06	..	0.00	..
	r.m.s.	0.10	0.28	..	0.13	..	0.16	..
5576 (A294)	u	+0.69	+1.27	+0.49	+0.86	+0.24	+0.19	..
	r.m.s.	0.29	0.54	0.45	0.30	0.39	0.20	..
	v	−0.41	+0.28	0.00	+0.41	−0.16	+0.40	..
	r.m.s.	0.19	0.26	0.34	0.40	0.22	0.12	..
	$W-W_0$	−0.24	−0.22	−0.18	−0.08	−0.20	0.00	..
	r.m.s.	0.05	0.08	0.11	0.08	0.06	0.03	..
5691 (A295)	u	+1.18	+2.39	+1.98	+1.85	+1.41	..	+0.34
	r.m.s.	0.95	0.52	0.70	0.54	0.71	..	0.57
	v	+0.20	+0.66	+0.27	+0.56	+0.37	..	+0.05
	r.m.s.	0.14	0.27	0.42	0.30	0.40	..	0.32
	$W-W_0$	+0.04	−0.14	−0.07	0.00	0.00	..	0.00
	r.m.s.	0.06	0.09	0.11	0.07	0.08	..	0.06

TABLE 4—(*Contd.*)

Component velocities in km/sec in Sunspot No. KKL .2375 on February 15, 1963 at $\mu = 0.75$

Spectral line used		Distance from the centre of the spot in 10^3 km.						
		4.37	5.12	5.87	6.62	7.37	8.13	8.87
4912 (A299)	u	+0.80	+1.00	+0.61	+1.42	+1.27	+1.74	+0.94
	r.m.s.	0.20	0.28	0.32	0.19	0.30	0.20	0.33
	v	−0.40	−0.17	−0.22	0.02	−0.11	+0.21	−0.55
	r.m.s.	0.02	0.19	0.26	0.22	0.22	0.03	0.21
	W−W_o	−0.26	−0.16	−0.19	−0.39	−0.30	−0.06	−0.01
	r.m.s.	0.09	0.10	0.16	0.10	0.11	0.01	0.10
5576 (A300)	u	+0.90	+1.05	+0.77	+0.47	+0.65	+0.55	+0.27
	r.m.s.	0.16	0.12	0.20	0.12	0.30	0.23	0.18
	v	+0.23	+0.33	−0.31	+0.17	+0.14	−0.11	+0.19
	r.m.s.	0.07	0.07	0.30	0.13	0.32	0.16	0.07
	W−W_o	−0.06	0.00	0.00	−0.08	+0.01	+0.02	+0.10
	r.m.s.	0.05	0.01	0.12	0.06	0.16	0.08	0.04
5691 (A301)	u	+1.03	+1.81	+1.55	+1.26	+0.90	+0.92	+1.11
	r.m.s.	0.33	0.03	0.88	0.17	0.42	0.14	0.02
	v	−0.24	+0.31	+0.09	−0.13	−0.14	+0.24	−0.01
	r.m.s.	0.21	0.42	0.54	0.25	0.30	0.14	0.24
	W−W_o	−0.10	+0.12	−0.09	+0.22	0.02	+0.18	−0.09
	r.m.s.	0.11	0.24	0.28	0.09	0.19	0.07	0.12

Spectral line used		Distance from the centre of the spot in 10^3 km.					
		9.62	10.50	11.10	11.80	13.20	15.00
4912 (A299)	u	+1.25	+1.98	+1.02	+0.02	+1.03	+0.00
	r.m.s.	0.63	0.40	0.20	0.09	0.55	0.25
	v	+0.01	+0.10	−0.30	−0.01	−0.17	+0.11
	r.m.s.	0.31	0.25	0.17	0.05	0.18	0.19
	W−W_o	−0.07	+0.06	−0.06	−0.02	−0.06	0.00
	r.m.s.	0.18	0.13	0.09	0.02	0.11	0.04
5576 (A300)	u	..	+0.59	+0.02	..	..	+0.38
	r.m.s.	..	0.30	0.27	..	..	0.26
	v	..	−0.07	−0.13	..	..	−0.07
	r.m.s.	..	0.14	0.11	..	..	0.12
	W−W_o	..	+0.06	+0.08	..	..	0.00
	r.m.s.	..	0.06	0.35	..	..	0.06
5691 (A301)	u	+1.31	+1.19	+0.92	..	+0.90	+0.65
	r.m.s.	0.42	0.21	0.18	..	0.22	0.14
	v	−0.03	+0.04	−0.19	..	−0.72	0.09
	r.m.s.	0.27	0.12	0.12	..	0.08	0.08
	W−W_o	−0.09	−0.02	−0.02	..	+0.34	0.00
	r.m.s.	0.18	0.06	0.06	..	0.54	0.40

TABLE 4—(*Contd.*)

Component velocities in km/sec in Sunspot No. KKL 12375 on February 16, 1963 at $\mu = 0.56$

Spectral line used		Distance from the centre of the spot in 10^3 km.					
		4.37	5.12	5.87	6.62	7.37	8.13
4912 (A305)	u	+1.09	+1.46	+1.11	+2.09	+1.77	+1.61
	r.m.s.	0.18	0.21	0.21	0.61	0.46	0.50
	v	+0.18	+0.25	−0.07	+0.62	+0.13	+0.21
	r.m.s	0.09	0.08	0.12	0.33	0.11	0.20
	W−W_0	−0.06	+0.02	−0.05	−0.28	−0.05	−0.03
	r.m.s.	0.06	0.05	0.05	0.19	0.07	0.10
5576 (A306)	u	+0.70	+0.68	+0.72	+0.76	+0.22	..
	r.m.s.	0.19	0.23	0.29	0.78	0.34	..
	v	+0.09	−0.03	+0.12	+0.16	−0.11	..
	r.m.s.	0.11	0.14	0.11	0.18	0.14	..
	W−W_0	−0.13	−0.13	−0.13	+0.01	−0.19	..
	r.m.s.	0.07	0.08	0.07	0.09	0.08	..
5691 (A307)	u	+1.70	+1.70	+1.89	+1.63	+2.00	+2.13
	r.m.s	0.34	0.37	0.58	0.40	0.62	0.41
	v	+0.30	+0.27	+0.37	+0.22	+0.14	+0.41
	r.m.s.	0.12	0.15	0.23	0.36	0.15	0.42
	W−W_0	−0.39	−0.30	−0.29	−0.25	−0.24	−0.08
	r.m.s.	0.08	0.08	0.12	0.16	0.10	0.16

Spectral line used		Distance from the centre of the spot in 10^3 km.				
		8.87	9.62	10.50	12.00	14.00
4912 (A305)	u	..	+0.24	+1.16	+1.22	+1.08
	r.m.s.	..	0.61	0.46	0.47	0.72
	v	..	−0.34	−0.02	+0.17	+0.10
	r.m.s.	.	0.20	0.14	0.18	0.19
	W− W_0	..	0.00	−0.04	−0.06	0.00
	r.m.s.	..	0.09	0.06	0.05	0.07
5576 (A306)	u	+0.69	+0.90	+0.59	+0.79	+0.84
	r.m.s.	0.50	0.37	0.32	0.09	0.59
	v	+0.30	+0.06	−0.12	0.00	+0.07
	r.m.s.	0.41	0.69	0.09	0.32	0.15
	W−W_0	0.00	−0.01	−0.01	−0.03	0.00
	r.m.s.	0.25	0.31	0.05	0.18	0.06
5691 (A307)	u	..	+1.95	..	+1.48	+0.87
	r.m.s.	..	0.15	..	0.50	0.10
	v	..	+0.26	..	+0.40	+0.24
	r.m.s.	..	0.01	..	0.19	0.51
	W−W_0	..	−0.27	..	0.00	0.00
	r.m.s.	..	0.09	..	0.07	0.34

TABLE 4—(*Contd.*)

Component velocities in km/sec in Sunspot No. KKL 12368 *on January* 20, 1963 *at* $\mu = 0.54$

Spectral line used		Distance from the centre of the spot in 10^3 km.				
		5.50	6.75	8.25	9.75	11.20
4912 (A186)	u	..	+0.06	+0.90	+1.04	+0.89
	r.m.s.	..	0.10	0.07	0.13	0.07
	v	..	+0.80	+0.55	+0.31	−0.04
	r.m.s.	..	0.12	0.08	0.08	0.10
	W − W_o	..	−0.29	−0.38	−0.24	−0.20
	r.m.s.	..	0.07	0.04	0.06	0.09
5576 (A181)	u	+0.20	+0.35	+0.22	+0.57	+0.40
	r.m.s.	0.05	0.08	0.11	0.14	0.19
	v	+0.19	−0.16	−0.12	−0.02	+0.13
	r.m.s.	0.05	0.08	0.10	0.20	0.19
	W − W_o	+0.03	+0.01	−0.06	−0.02	−0.07
	r.m.s.	0.02	0.04	0.06	0.10	0.11
5691 (A180)	u	+0.28	+0.47	+0.66	+0.62	+0.65
	r.m.s.	0.04	0.23	0.14	0.27	0.21
	v	−0.06	+0.52	+0.17	+0.29	−0.06
	r.m.s.	0.04	0.22	0.19	0.29	0.22
	W − W_o	−0.21	0.00	0.00	−0.03	+0.16
	r.m.s.	0.01	0.03	0.10	0.16	0.14

Spectral line used		Distance from the centre of the spot in 10^3 km.				
		12.70	14.20	15.70	17.20	18.70
4912 (A186)	u	+1.03	+0.79	+0.79	+0.56	+0.54
	r.m.s.	0.21	0.12	0.42	0.31	0.51
	v	+0.31	−0.14	+0.51	+0.13	−0.08
	r.m.s.	0.20	0.18	0.39	0.50	0.48
	W − W_o	−0.11	−0.12	−0.12	0.00	0.00
	r.m.s.	0.09	0.07	0.20	0.11	0.22
5576 (A181)	u	+0.53	+1.00	+0.52	+0.47	+0.43
	r.m.s.	0.16	0.24	0.18	0.14	0.21
	v	+0.17	+0.43	+0.18	+0.18	+0.07
	r.m.s.	0.20	0.17	0.25	0.29	0.20
	W − W_o	−0.08	−0.08	+0.09	0.00	0.00
	r.m.s.	0.10	0.07	0.10	0.06	0.07
5691 (A180)	u	+0.74	+0.69	+0.77	+0.45	+0.72
	r.m.s.	0.29	0.08	0.38	0.21	0.22
	v	−0.06	−0.68	0.00	−0.94	+0.28
	r.m.s.	0.22	0.05	0.28	0.57	0.20
	W − W_o	+0.18	−0.28	+0.18	−0.31	0.00
	r.m.s.	0.14	0.08	0.12	0.12	0.09

TABLE 4—(*Contd.*)

Component velocities in km/sec Sunspot No. KKL 12368 *on January* 21, 1963 *at* $\mu = 0.35$

Spectral line used		Distance from the centre of the spot in 10^3 km.				
		5.50	6.75	8.25	9.75	11.20
4912 (A189)	u	+0.69	+0.40	+0.66	+0.38	+0.31
	r.m.s.	0.16	0.16	0.13	0.21	0.22
	v	+0.13	−0.08	+0.02	−0.12	−0.18
	r.m.s.	0.19	0.14	0.08	0.22	0.30
	W−W$_o$	−0.17	−0.21	−0.02	−0.08	−0.07
	r.m.s.	0.07	0.08	0.05	0.00	0.08
5576 (A190)	u	+0.59	+0.45	+0.44	+0.51	+0.62
	r.m.s.	0.19	0.14	0.13	0.14	0.26
	v	+0.25	+0.24	+0.32	+0.11	+0.31
	r.m.s.	0.14	0.13	0.21	0.13	0.17
	W−W$_o$	+0.13	−0.08	−0.04	0.00	0.00
	r.m.s.	0.09	0.07	0.09	0.04	0.09
5691 (A191)	u	+0.91	+0.80	+0.82	+0.96	+0.61
	r.m.s.	0.09	0.12	0.19	0.11	0.19
	v	+0.52	+0.35	+0.38	+0.39	+0.33
	r.m.s.	0.00	0.11	0.22	0.28	0.16
	W−W$_o$	+0.09	0.00	+0.01	0.00	−0.08
	r.m.s.	0.05	0.08	0.15	0.12	0.09

Spectral line used		Distance from the centre of the spot in 10^3 km.				
		12.70	14.20	15.70	17.20	19.00
4912 (A189)	u	+0.58	..	+0.08	..	..
	r.m.s.	0.13	..	0.10	..	..
	v	+0.24	..	−0.19	..	..
	r.m.s.	0.12	..	0.08	..	..
	W−W$_o$	+0.08	..	0.00	..	..
	r.m.s.	0.01	..	0.02	..	..
5576 (A190)	u	+0.22	..	+0.32	+0.23	+0.16
	r.m.s.	0.24	..	0.18	0.23	0.18
	v	−0.13	..	0.00	+0.03	+0.05
	r.m.s.	0.19	..	0.14	0.18	0.15
	W−W$_o$	+0.09	..	+0.06	+0.02	0.00
	r.m.s.	0.06	..	0.05	0.05	0.08
5691 (A191)	u	+0.85	+0.49	..	+0.31	+0.08
	r.m.s.	0.27	0.24	..	0.23	0.11
	v	+0.09	+0.19	..	+0.14	−0.01
	r.m.s.	0.90	0.17	..	0.16	0.09
	W−W$_o$	+0.02	+0.05	..	−0.01	0.00
	r.m.s.	0.13	0.06	..	0.06	0.05

The run of the radial velocity u, shows that the radial velocity steeply increases near the umbral border, to attain its maximum value near the middle of the penumbral region. From the peak value, the radial velocity gradually declines to become nearly zero, far out in the photosphere. Recently Brekke and Per Maltby (1963) have shown, from observations of a single spot that the radial velocities abruptly cease at the outer boundary of the penumbra. However, observations of Evershed (1916), Kinman (1952, 1953), Holmes (1961), Servajean (1961) and this study, show that the material flow continues far out into the photosphere.

The rise of the radial velocity to the peak value is generally very steep compared to the decline. A slight shift in the location of the peak velocity across the penumbra could be due to the errors in locating the boundaries of the umbra and the penumbra. The magnitude of the maximum radial velocity U_{max} in all the three lines, shows a decrease towards the disk positions of the spot near the limb. Michard (1951) and recently Servajean (1961) have reported such a decrease of U_{max} near the limb position and have interpreted this decrease as due to the decrease of U_{max} with increasing height in the photosphere. Holmes (1963a) has shown that the observed velocities in spots are affected more towards the limb by the scattered light and the observed decrease of U_{max} may not wholly be due to the level difference in the photosphere. A plot between U_{max} and the disc positions, for each of the three lines, is given in Figure 5. The slope of U_{max} : μ for 5691 and 4912 lines is almost the same, while for the stronger line 5576 (Rowland intensity 4) the slope is different. The 5576 line is formed at a higher level than either of the two lines.

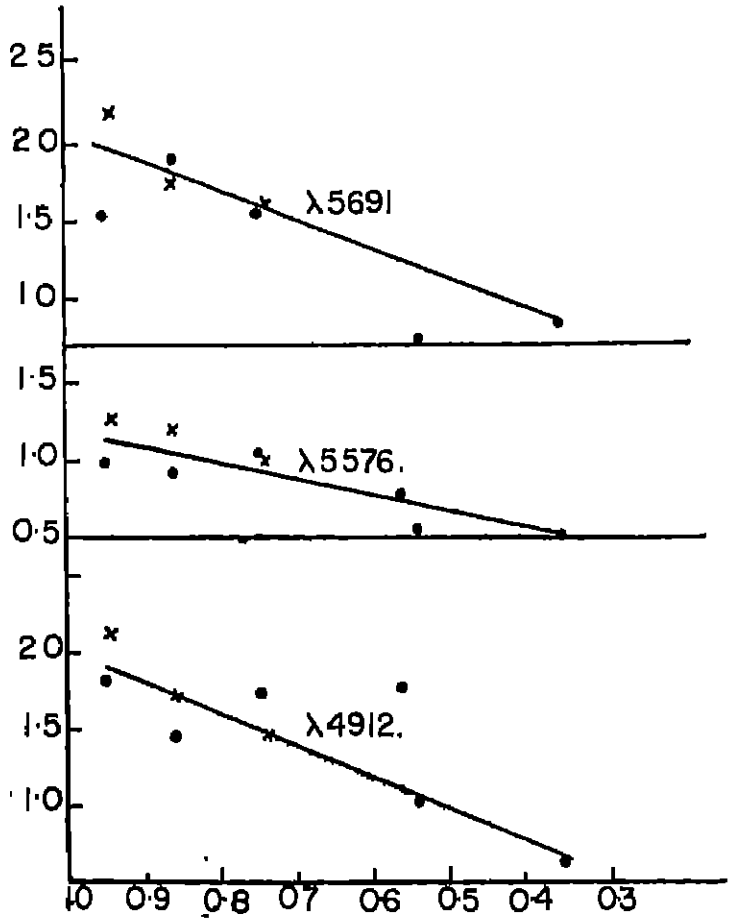

Figure 5.—U_{max} versus disc position (μ) of spots. Crosses indicate the velocities measured in the eastern quadrant; dots indicate the velocities measured in the western quadrant.
Ordinate — U_{max} in Km/sec. Abscissa — disc position of the spot.

Comparing the pattern of radial velocity curves for different disc positions of the spot, it is noticed that the velocity patterns flatten out for, the spot-positions near the limb. For spots located near disc centre, the radial velocity curves show a steep rise and relatively slow decline. The velocity run for all the three lines at one disc position appears to be similar. On some disc positions of the spot, a small hump appeared near the outer edge of the penumbra. This hump in velocity curve was visible in all the three lines. A similar double peak in the radial velocity curve was also observed by Kinman (1953) in the case of Mount Wilson spot No. 10955. Sunspot spectra obtained on January 20 (μ=0.54) and February 16 (μ=0.54) refer to the same spot group, but on two different passages and almost at the same central meridian distance. Hence the velocity fields obtained on January 20 and February 16 can be compared for possible effects of age difference. These observations reveal that the spots show large radial velocities during their well developed phase, compared to the early phases.

Comparing the radial velocity field and the magnetic field maps, it is evident that the radial velocity increases in the penumbra with increasing distance from the umbral border. The velocity attains its maximum value about half way in the penumbral region, and then gradually decreases to zero well outside the penumbral limit. The magnetic field however, decreases monotonically with increasing distance from the spot centre to attain less than or equal to half its peak value near the middle of the penumbra. In this study of the Evershed effect and the spatial magnetic field, it was not possible to obtain a point-to-point correlation between the velocity and magnetic field pattern. It is planned to investigate the interaction of magnetic and velocity fields in the sunspot atmosphere from the observations of high resolution spatial magnetic and velocity fields.

The variation of the maximum radial velocity U_{max} with depth in spots was first suggested by Evershed (1910) and later a detailed investigation was made by St. John (1913). From the calculations of the mean depth of formation of lines, gradients of U_{max} with depth were obtained at nine disc positions of the spot and are given in Table 3.

(b) *Vertical velocity*, w ; The vertical velocity w, is the component directed outwards and normal to the solar surface. The measures of the vertical velocity are referred to the vertical velocity w_0, of a far removed point in the photosphere. The quantity ($w-w_0$) and their r.m.s. errors are plotted in the lower halves of Figure 4. The direction of these small vertical velocities is systematically negative in the penumbra and the maximum amplitude is of the order of—0.3 km/sec. This indicates a descending motion of matter, in the penumbral region.

The variation of the vertical velocity with disc position is evident from Table 3. A decrease of maximum vertical velocity towards the limb positions of the spot, is observed for all the three lines.

(c) *Tangential velocity*, v ; The existence or otherwise of the tangential component of velocity or a rotational motion, in sunspots is yet to be confirmed. There are reliable and convincing observations in the literature that indicate the presenceas well as absence of the tangential velocities in sunspots. Evershed (1910, 1916) detected tangential velocities of the order of 0.25 to 0.35 km/sec and even higher. Abetti (1932) found irregular tangential velocities of the order of 0 to 5 km/sec and suggested that the tangential motion varied from spot to spot. Kinman (1952) found that the the tangential component v was random in nature and was well within the errors of measurements. Servajean (1961) has also shown that the magnitude of v, on most of the spot positions on the disc was very small. In his Table III (Servajean 1961) sizable tangential velocities (– 0.33 to +0.55 km/sec) occur on April 27 and 30.

Our results of the tangential velocities and their r.m.s. errors, are given in Table 3. Figure 6 shows the run of tangential velocity component and their r.m.s. errors, on February 9 and 10, measured in all three lines. The tangential velocity measured from the spectra of January 20, 21 and February 9 & 10, show a slight systematic pattern of velocity variation over and above the large r.m.s. errors. At positions near the disc centre, the tangential velocity patterns show no systematic trend. At a few points in the spot, the component velocity v was found to be as high as 1.5 ±0.6 km/sec. An exact correspondence between the tangential velocity run in all the three lines is not found.

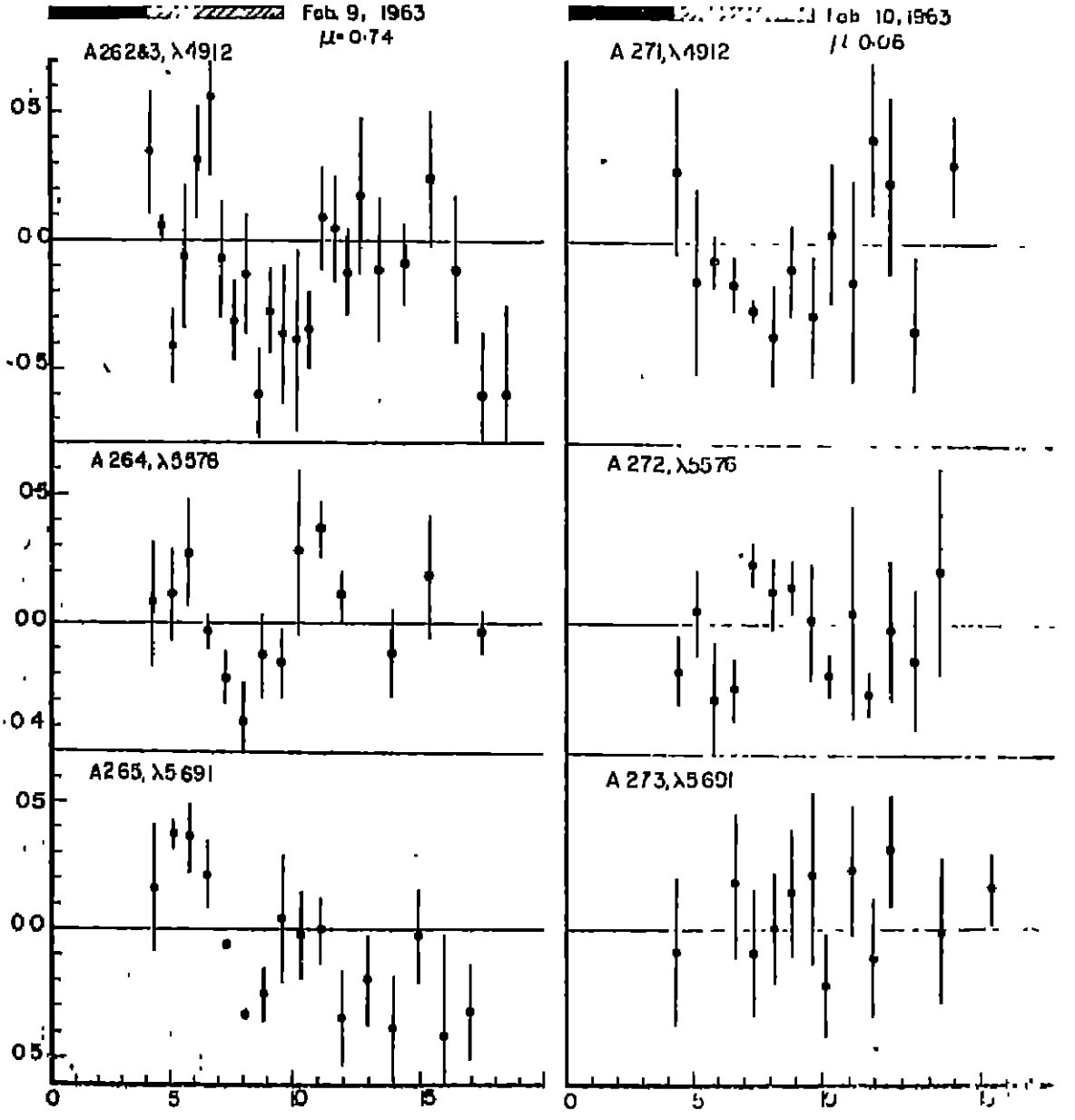

Figure 6.—Run of tangential velocity component and r.m.s errors.
Ordinate — in km/sec
Abscissa — in 1000 km

From our observations of the tangential velocity and also on the basis of the work briefly reviewed earlier, it will be realized that further observational corroboration is necessary before we can definitely recognize the contribution of the tangential component to the velocity fields in sunspots. Adam's (1963) recent measures of the magnetic field in spots and the detection of the azimuthal component of magnetic field indicate the possibility of the presence of tangential and vertical velocities. Adam (1963) has shown that while the field strength remains stable, the direction of magnetic field varies from day to day.

As shown earlier, the largest contribution to the mass motion in spot penumbra comes from the radial component only. Nevertheless, the existence of the tangential motion has not been repudiated and on the other hand its presence may be in agreement with the recent observations of Adam (1963). Considering the high conductivity of the solar material, the flow of material has to be along the magnetic lines of force. It would be impossible for the conducting material to 'slip-cross' perpendicularly the magnetic lines of force. With the existence of the azimuthal component of magnetic field in sunspot penumbrae, it implies that the motion should have a tangential component also.

In some of the radial and tangential velocity measures, large r.m.s. errors are noticed. These large r.m.s. errors could be due to the following reasons ;

(1) the number of the measured velocity points in each annular zone may be small,

(2) our basic assumption that the motion has a cylindrical symmetry about the centre of the spot, may not be wholly valid.

The phenomenon of line profile asymmetry in sunspot penumbrae.: The important phenomenon of asymmetry of spectral lines in the sunspot penumbral regions, was first discovered by Evershed (1916). He showed that near the outer boundary of a spot penumbra, the spectral lines develop a strong diffuse wing, which is always directed towards the Evershed displacement. A diffuse asymmetric wing in lines is easily seen on the spot spectra taken by McMath et al. (1956). Recently, Bumba (1960) at the Crimean Observatory has studied this phenomenon. He used high spectrographic dispersion and a large solar image. He termed this diffuse asymmetry in spectral lines as 'Flag' and has resolved this 'Flag' into a separate 'Satellite' line. This satellite line indicates Doppler shifts of the order of 5 km/sec or more. Servajean (1961) has studied changes in the asymmetric nature of lines in the spot region and also at different spot locations on the solar disk. It seems that Bumba (1960), Servajean (1961) and other workers in reporting the phenomenon of asymmetry in sunspot lines seem to have overlooked its first discovery by Evershed in 1915. It is remarkable for Evershed (1916) to have observed the diffuse wing in lines near the penumbral region, even though he had at his disposal a small solar image (44 mm diameter) and relatively low spectrographic dispersion.

Observations and the photometric analysis of the line asymmetry: Some of the best spectra were selected from a collection of spot spectra for a detailed photometric study of the variation of the line asymmetry; (1) over the spot region, (2) with the location of spot on the disc, (3) at two places on the line profile and (4) with the strength of the line. A term "flag factor (F.F.)" is defined as a measure of the asymmetry in a line, and is given by

$$F.F. = (\lambda_1 - \lambda_0)$$

where λ_0 is the wavelength of the central intensity point and λ_1 is the wavelength of the centre of the line joining equal intensity points on the line profile. The flag factor' F.F., is measured at half intensity and at one-tenth intensity points on the line profile.

The spectra obtained under good seeing conditions on February 9 at L-Lo --39°.0 E., on February 12 at L--Lo=0°: and on February 15 at L—Lo=39°..0.W, in the threespectral regions 4912, 5576 and 5691 were used for this study. For the spatial variation of F.F. over the spot region, three slit positions, crossing the umbra centrally and on either sides of the umbra crossing only the penumbra were used. These three slit positions for the three disc posi ions of the spot, yield a picture that is very representative of the spatial aspect of the line asymmetry in spots. All the spectrograms used were calibrated with the aid of a Hilger step wedge filter. Microphotometer scans of the three Zeoman insensitive lines (4912 ;027, 5571·101 and 5691.508) were obtained at several places in the spot region and at a point far removed from the spot in the photosphere. The chart speed was adjusted to give a magnification of 25 times, thus yielding a dispersion of about 200 mm per Å on the traces. The positions of the scanned regions on the spot spectrum were determined using the wire shadows, registered while obtaining the spot spectra. The microphotometer scanning slit used was about 0".8 of arc in height and 0".3 of arc in width on the solar disk.

On six spectrograms and for one slit position, line profiles were obtained for 4912·027 and 5691.508 lines. These are given in Figure 7, as representative of some typical asymmetric line profiles. The 'flag factors' were determined at one-half and one-tenth intensity points on the line profile. Figure 8 gives the variation of flag factor in milliangstrom, over the spot region, in all the three lines (except for spectra obtained on February 9), and in three slit positions. In these figures the positions of spot and the slit are given to indicate the approximate location of the slit orientation and also the sight-line velocities measured along the length of the slit. The positive values of F.F., indicate flagging towards the long wavelength side, while the negative values indicate flagging towards the short wavelength side. The line profiles given are not corrected for the errors introduced by the instrumental profile of the 18-metre Littrow spectrograph. Using an Iodine absorption tube, it was found that the instrumental profile of this spectrograph is very narrow (less than 12 mÅ) and fairly symmetrial.

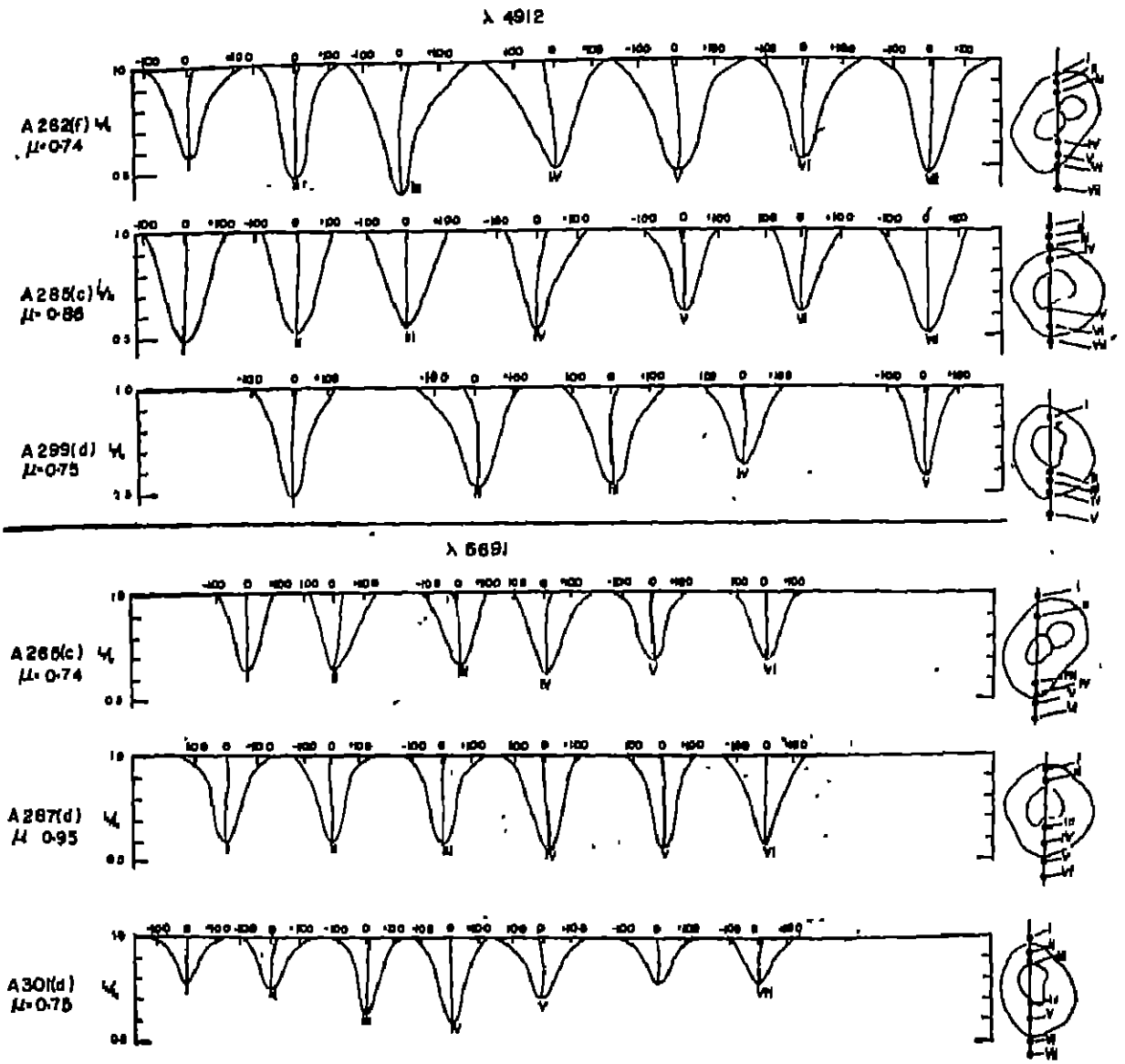

Figure 7—Variation of line profiles in sunspots.

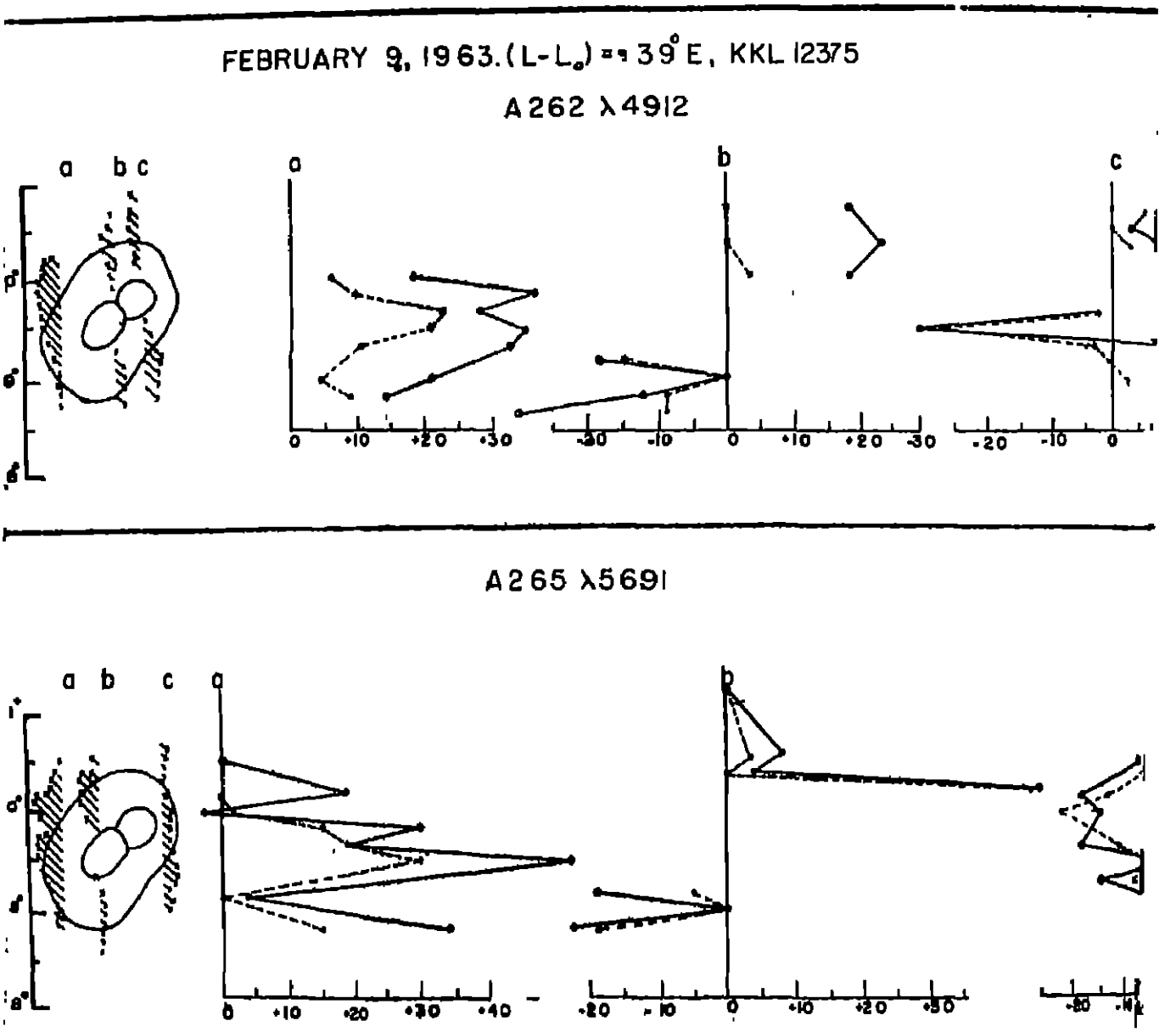

Figure 8 (a)—Variation of 'Fing factor' in sunspots, in units of milliangstrom. The sight-line velocities are indicated on the left.

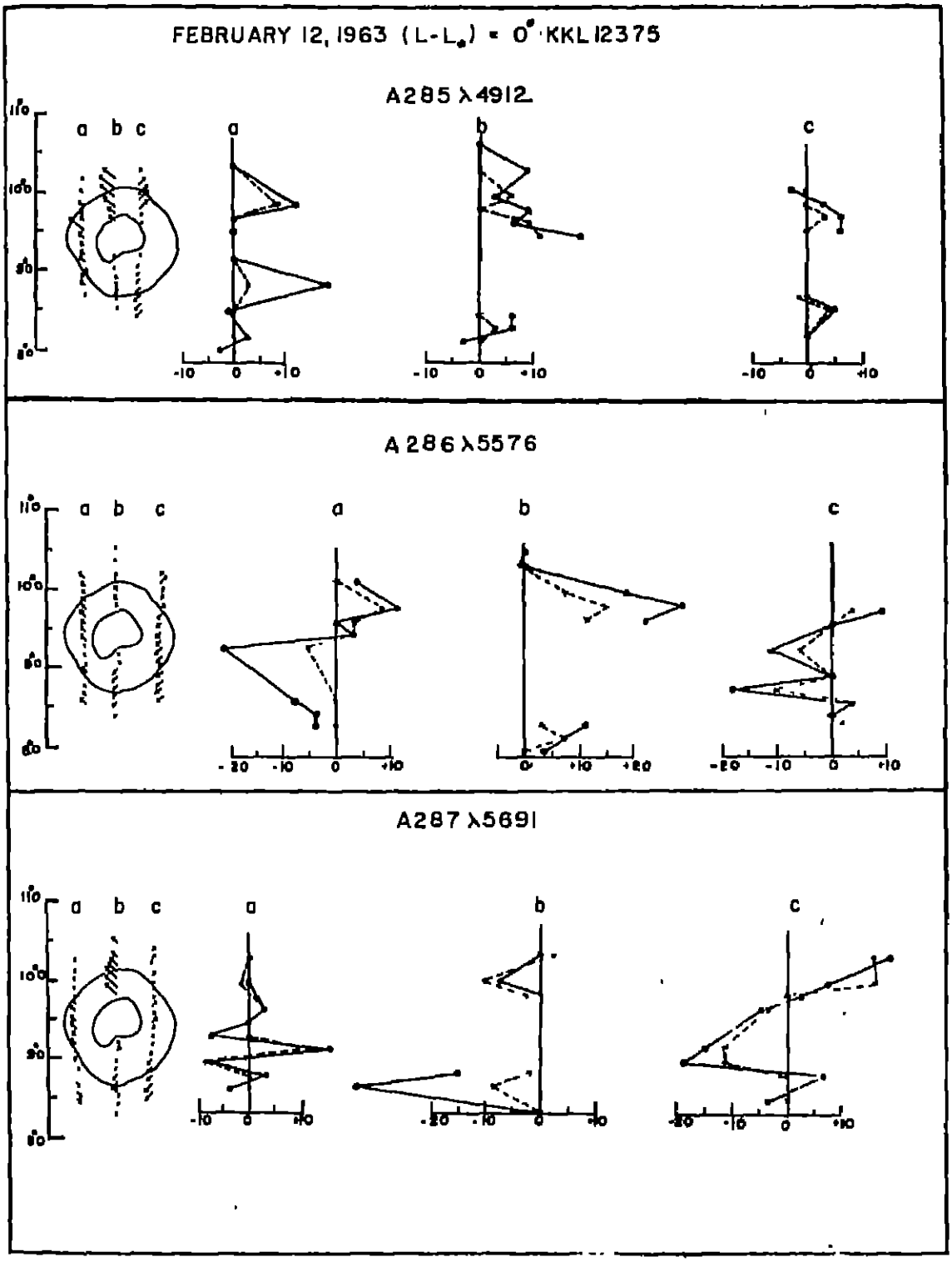

Figure 8 (b)—Variation of 'Flag factor' in sunspots, in units of milliangstroms. The sight-line velocities are indicated on the left.

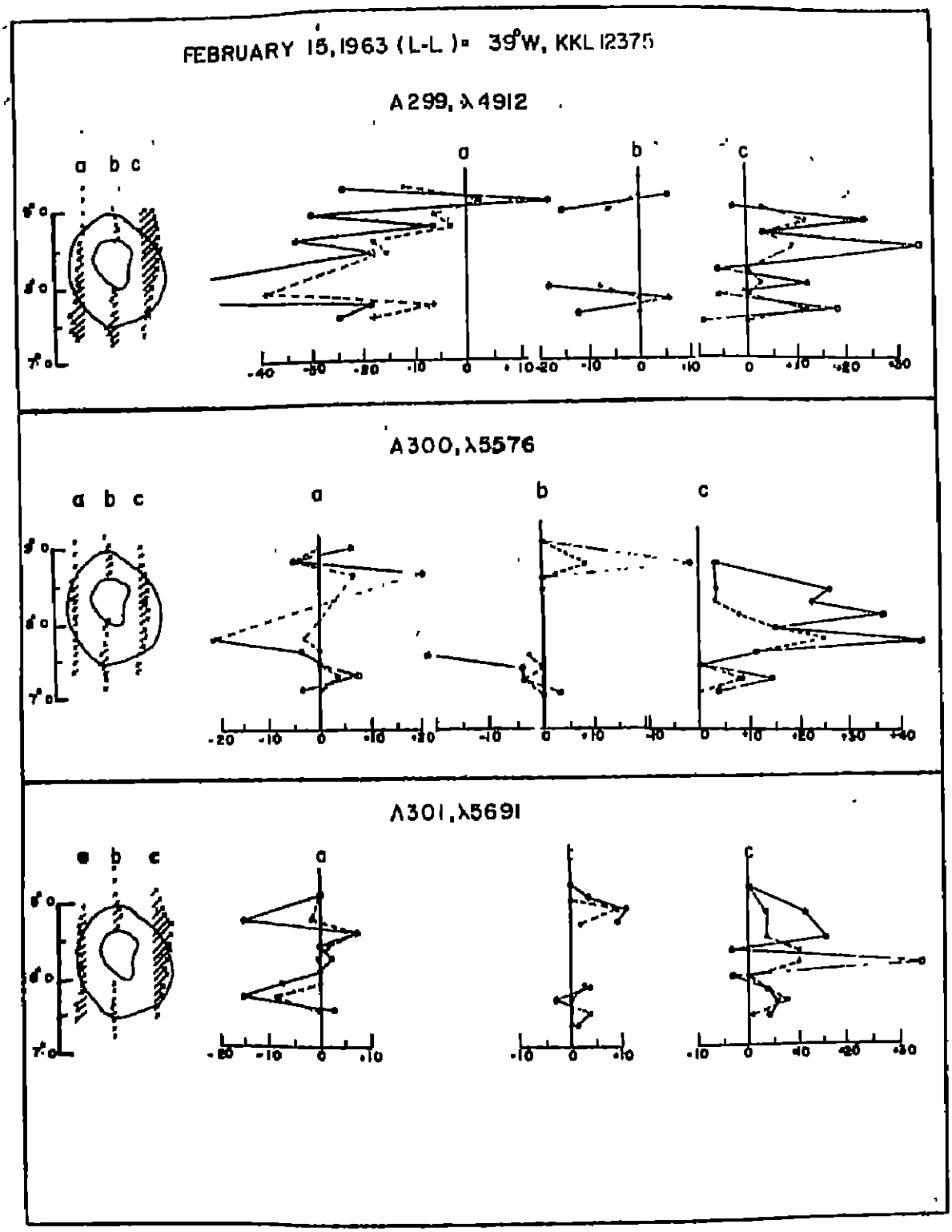

Figure 8 (c).—Variation of 'Flag factor' in sunspots, in units of milliangstrom. The sight-line velocities are indicated on the left.

Discussion of the line asymmetry ; From the 'flag factor' plots and the variation of the line profiles, it is noticed that the line profiles in the photosphere are symmetrical. In the region of the penumbra, the asymmetry increases to attain its maximum value around the middle of penumbral region. The magnitude of the 'flag factor' fluctuates considerably in the penumbral region. In some spot regions maximum asymmetry of about 60 mÅ at one-tenth central dip is noted. The maximum 'flag-factor' is a function of the disc position of the spot. In spot positions near the disc centre, the value of maximum 'flag-factor' is smaller compared to the spots near the limb. A variation of the 'flag factor' is noted with line strength. The 5576 line shows systematically a smaller 'flag factor' compared to the weaker lines, λ 4912 and λ 5691. A visual examination of some spot spectra taken by Dr. M.K.V. Bappu, at the Kitt Peak National Observatory, Arizona, using a large solar image (33 inches in diamter) and a spectrographic dispersion of 12 mm/Å, indicates a decrease in flagging with increasing line strength. The 4903 and 4919 lines of Rowland intensity 5 and 6, show marked decrease in asymmetry, compared to the weaker lines. The direction of flagging in the strong and weak lines is the same and in no case the flagging extends beyond the penumbral limit.

The spot spectra obtained at Kodaikanal and those obtained at Kitt Peak, under good to very good seeing conditions, do not show any indication of satellite line, as reported by Bumba (1961, 1963). The diffuse wing always appears to be joined with the parent line. Perhaps the appearance of the faint satellite line depends on some other rigorous factors of observation.

Some of the spectra obtained under extremely fine seeing conditions show brightness variation in the penumbral region. The 'flagging' in lines occur more conspicuously in the darker regions of the penumbra. In the brighter regions the lines appear, more or less symmetrical. It seems that the agency responsible for the asymmetry or flagging in lines is more efficient in the darker (cooler) penumbral regions, compared to the brighter (hotter) penumbral regions.

From the asymmetric appearance of the line profiles and their variation in the spot region it seems that this phenomenon is associated with velocity fields, either on the surface or deep in the sunspot atmosphere. Two plausible explanations have been put forward, one by Servajean and the other by Bumba. Servajean (1961) has suggested that asymmetry occurs due to the difference in velocities of different strata in the line forming layers while Bumba (1963) suggests, an upstreaming of material at the umbral-penumbral boundary, which bends to become horizontal in the penumbral region and turns downwards again near the outer penumbral border. It appears that the line asymmetries inthe penumbra may be due to the velocity fields of some kind. It was noted earlier that the flagging is always directed towards the general Evershed flow. Therefore it seems that the motion responsible for the asymmetry in lines is an additional motion superimposed on the Evershed flow. This additional motion in various layers, responsible for the asymmetry in lines, perhaps ceases abruptly at the outer boundary of the penumbra, while the Evershed flow continues well out into the photospheric region.

Diffuse wing in lines in the Photospheric regions; A similar phenomenon of diffuse asymmetric wings in lines as that observed in the penumbral region, is noticed in the photospheric region also. On our best spectra that show, "wiggles' due to the solar granulation, one can see slight diffusion or 'flaring' in one of the wings of Fraunhofer lines. A diffuse wing develops invariably in the same direction, as the Doppler displacement due to the granular motion and in the darker (cooler) regions of the spectrum. In the brighter (hotter) photospheric regions, the lines appear symmetrical and also slightly narrow. A detailed quantitative analysis of this phenomenon is required. Servajean (1961) has also reported the presence of a similar phenomenon in granulation spectra.

Acknowledgements : The author is greatly indebted to Dr. M.K. Vainu Bappu Director, Astrophysical Observatory, Kodaikanal, for suggesting this problem and for constant encouragement and guidance. The author wishes to thank Miss. N. Subrahmanyan, for stimulating dicussions and for the cooperation during this investigation. The work reported in this paper was done during the tenure of the author as a Senior Research Fellow of the Ministry of Education, Government of India.

KODAIKANAL OBSERVATORY,
November, 1966.

REFERENCES

Abetti, G. 1932, Mem. Soc. Astr. Ital., 6, 353.
Adam, M. G. 1963, M. N. **126**, 135.
Brekke, K., and Maltby, P. 1963, Ann. Astr. **26**, 383.
Bruggencate, P. ten, Lust, Kulka, R., and Voight, H. 1955, Veroffentlichungen der Universitats-Sternwarte zu Gottingen, No. 110.
Bumba, V. 1960, Izvestiya Krym, Astro. Obs., **23**, 253.
Bumba, V. 1963, B. A. C., **14**, 1937.
Calami, G. 1934, Oss. Mem. Arcetri, **52**, 39.
Evershed, J. 1909a, M. N. **69**, 454.
Evershed, J. 1909b, Bull. Kodaikanal Obs. **2**, No. 15, 63.
Evershed, J. 1909c, Mem. Kodaikanal Obs., **1**.
Evershed, J. 1909d, The Observatory, **32**, 291.
Evershed, J. 1910, M. N. **70**, 217.
Evershed, J. 1913, Bull. Kodaikanal Obs., **3**, No. 32, 17.
Evershed, J. 1916, Bull. Kodaikanal Obs., **3**, No. 51, 167.
Edmonds, F. N. 1962, Ap. J., **136**, 507.
Goldberg, L., Muller, E. A., and Aller, L. H., 1960, Ap. J., Suppl. 5, 1.
Holmes, J. 1961, M. N., **122**, 301.
Holmes, J. 1963a, The Observatory, **86**, 163.
Holmes, J. 1963b, M. N. **126**, 155.
Kinman, T. D. 1952, M. N., **112**, 425.
Kinman, T. D. 1953, M. N., **113**, 613.
Makita, M. 1963, Pub. Astr. Soc. Japan, **15**, 145.
McMath, R. R., Mohler, O. C., Pierce, A. K., and Goldberg, L. 1956, Ap. J., **124**, 1.
Michard, R. 1951, Ann. Astr. **14**, 101.
Minkowski, R. 1942, Ap. J., **96**, 306.
Pierce, A. K., and Waddell, J. H. 1961, Mem. R. A. S., **68**, 89.
Plaskett, H. H. 1952. M. N., **112**, 414.
Servajean, R. 1961, Ann. Astr., **24**, 1.
St. John, C. E. 1913, Ap. J., **37**, 322.
Walker, G. T. 1909, Bull. Kodaikanal Obs. 2, No. **16**, 71.
Wright, K. O. 1944, Ap. J., **99**. 249.

MGIPCBE—82—10 DAOK/66—27-4-68—400